LAPPEENRANTA UNIVERSITY OF TECHNOLOGY
Faculty of Technology
Energy Technology

Seppo Koivuranta

GAMMA SPECTROMETRY AND GAMMA AND X-RAY TOMOGRAPHY OF NUCLEAR FUEL

Examiners and instructors: Professor Riitta Kyrki-Rajamäki
PhD Petri Kotiluoto

ABSTRACT

Lappeenranta University of Technology
Faculty of Technology
Energy Technology

Seppo Koivuranta

Gamma spectrometry and gamma and X-ray tomography of nuclear fuel

Master's thesis

2009

81 pages, 41 figures and 4 tables

Examiners: Professor Riitta Kyrki-Rajamäki
PhD Petri Kotiluoto

Keywords: gamma spectrometry, gamma tomography, X-ray tomography, nuclear fuel

The purpose of gamma spectrometry and gamma and X-ray tomography of nuclear fuel is to determine both radionuclide concentration and integrity and deformation of nuclear fuel.

The aims of this thesis have been to find out the basics of gamma spectrometry and tomography of nuclear fuel, to find out the operational mechanisms of gamma spectrometry and tomography equipment of nuclear fuel, and to identify problems that relate to these measurement techniques.

In gamma spectrometry of nuclear fuel the gamma-ray flux emitted from unstable isotopes is measured using high-resolution gamma-ray spectroscopy. The production of unstable isotopes correlates with various physical fuel parameters.

In gamma emission tomography the gamma-ray spectrum of irradiated nuclear fuel is recorded for several projections. In X-ray transmission tomography of nuclear fuel a radiation source emits a beam and the intensity, attenuated by the nuclear fuel, is registered by the detectors placed opposite. When gamma emission or X-ray transmission measurements are combined with tomographic image reconstruction methods, it is possible to create sectional images of the interior of nuclear fuel.

MODHERATO is a computer code that simulates the operation of radioscopic or tomographic devices and it is used to predict and optimise the performance of imaging systems. Related to the X-ray tomography, MODHERATO simulations have been performed by the author.
Gamma spectrometry and gamma and X-ray tomography are promising non-destructive examination methods for understanding fuel behaviour under normal, transient and accident conditions.

TIIVISTELMÄ

Lappeenrannan teknillinen yliopisto
Teknillinen tiedekunta
Energiatekniikka

Seppo Koivuranta

Ydinpolttoaineen gammaspektrometria sekä gamma- ja röntgentomografia

Diplomityö

2009

81 sivua, 41 kuvaa ja 4 taulukkoa

Tarkastajat: Professori Riitta Kyrki-Rajamäki
FT Petri Kotiluoto

Hakusanat: gammaspektrometria, gammatomografia, röntgentomografia
Keywords: gamma spectrometry, gamma tomography, X-ray tomography

Ydinpolttoaineen gammaspektrometrian sekä gamma- ja röntgentomografian tarkoituksena on määrittää ydinpolttoaineessa olevien radioaktiivisten aineiden koostumus sekä ydinpolttoaineen eheys ja säteilytyksen aiheuttamat muodonmuutokset.

Työn tarkoituksena on ollut selvittää ydinpolttoaineen gammaspektrometrian sekä gamma- ja röntgentomografian perusteet sekä mittausmenetelmien toimintaperiaate ja tunnistaa niihin liittyviä ongelmia ja esittää ratkaisuehdotuksia.

Ydinpolttoaineen gammaspektrometriassa hyödynnetään säteilytetyn polttoaineen emittoimaa gammasäteilyä. Tiettyjen radioaktiivisten nuklidien emittoima gammasäteily on verrannollinen polttoaineen fyysisiin ominaisuuksiin.

Ydinpolttoaineen gammaemissiotomografiassa säteilytetyn ydinpolttoaineen emittoima gammasäteily mitataan useasta suunnasta. Vastaavasti ydinpolttoaineen transmissiotomografiassa ydinpolttoaine on asetettu ulkoiseen röntgensäteilykeilaan ja säteilyn vaimeneminen mitataan läpivalaisukeilan vastakkaiselta puolelta säteilynilmaisimilla. Mittauksista saadun datan ja tomografisten kuvarekonstruktiomenetelmien avulla voidaan luoda paikallisia poikkileikkauskuvia ydinpolttoaineen sisustasta.

MODHERATO on tietokonekoodi jota käytetään simuloimaan radioskopisia ja tomografisia laitteistoja. Työn tekijä on tehnyt simulointeja MODHERATO koodilla ja tulokset on esitetty työssä.

Gammaspektrometria sekä gamma- ja röntgentomografia ovat lupaavia ainetta rikkomattomia tutkimusmenetelmiä ydinpolttoaineen käyttäytymisen ymmärtämiseksi normaali-, transientti- ja onnettomuustilanteissa.

ABBREVIATIONS

ADC	Analog-to-digital Converter
ART	Algebraic Reconstruction Technique
BGO	Bismuth Germanate
BU	Burnup
BWR	Boiling Water Reactor
CCD	Charge-coupled Device
CdTe	Cadmium Telluride
CEA	Commissariat à l'Énergie Atomique
	French Atomic Energy Commission
Clab	Centralt mellanlager för använt kärnbränsle
	The Swedish interim storage for spent nuclear fuel
CZT	Cadmium-zinc-telluride
DC	Direct Current
DSP	Digital Signal Processing
FBP	Filtered Backprojection
FGR	Fission Gas Release
GaAs	Gallium Arsenide
HgI_2	Mercuric Iodide
HPGe	High-purity Germanium
IAEA	International Atomic Energy Agency
JHR	Jules Horowitz Reactor
LWR	Light Water Reactor
MCNP	Monte-Carlo N-Particle Transport Code
MODHERATO	Modélisaton Haute Energie pour la Radiographie et la Tomographie
	Modelling High Energy Radiation Tomography
NaI	Sodium Iodine
NDE	Non-destructive Examination
NDT	Non-destructive Testing
NMR	Nuclear Magnetic Resonance
PET	Photon Emission Tomography
PWR	Pressurized Water Reactor
RF	Radio Frequency

SPECT	Single Photon Emission Computed Tomography
SKB	Svensk Kärnbränslehantering AB Swedish Nuclear Fuel and Waste Management Company
STUK	Säteilyturvakeskus Radiation and Nuclear Safety Authority
TOF	Time-of-flight
VTT	Technical Research Centre of Finland

1. Introduction

One of the main challenges of the nuclear power safety concerns the safety of nuclear reactors in both normal operation and severe accident conditions. In the nuclear fuel research, gamma spectrometry, X-ray radiography, and gamma- and X-ray tomography can be used to study both radionuclide concentrations and integrity and deformation of nuclear fuel.

Technical Research Centre of Finland (VTT) and Commissariat à l'Énergie Atomique (CEA) are co-operating in Jules Horowitz Reactor project. Jules Horowitz Reactor is a material testing reactor that is been built in Cadarache, France. The reactor will be used mainly for fuel studies and material testing. One of the VTT's tasks is to design and deliver a gamma spectrometry and tomography equipment which will be used in fuel studies.

The aims of this thesis are to find out the basics of gamma spectrometry and tomography of nuclear fuel, find out the operational mechanisms of gamma spectrometry and tomography equipment of nuclear fuel and identify problems that relate to these measurement techniques. VTT has no earlier experience about tomography of nuclear fuel so it is emphasized in this thesis.

1.1 Electromagnetic radiation

Electromagnetic radiation is a self-propagating wave in space with electric and magnetic components. These components oscillate at right angles to each other and to the direction of propagation, and are in phase with each other. Any electromagnetic radiation can be described in terms of its wavelength λ, its frequency v, or the equivalent energy E. Electromagnetic radiation is traditionally classified into types according to the frequency of the wave: these types include, in order of increasing frequency, radio waves,

microwaves, terahertz radiation, infrared radiation, visible light, ultraviolet radiation, X-rays and gamma-rays. The range of electromagnetic radiation is shown in Figure 1.1.

However, in more recent literature, the classification of X-rays and gamma radiation is made on the basis of origin, that is: the electromagnetic radiation originating from nuclear decay is classified to be gamma radiation and electromagnetic radiation originating from transitions of electrons between different atom shells or from charged particle Bremsstrahlung, is called X-rays.

Gamma- and X-rays are a form of ionizing radiation. Ionizing radiation is a radiation with enough energy so that during an interaction with an atom, it can remove tightly bound electrons from the orbit of an atom, causing the atom to become charged or ionized.

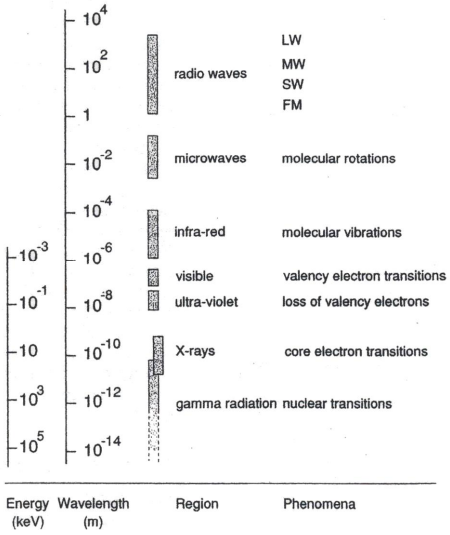

Figure 1.1 The range of electromagnetic radiation. [2]

1.2 X-rays

Characteristic X-rays are electromagnetic radiation that is emitted in transitions of the atomic electrons between different states in atom. The basic

production of X-rays is by accelerating electrons in order with a metal target, for example anode of X-ray tube. The electrons suddenly decelerate upon colliding with the metal target and if enough energy is contained within the electron it is able to knock out an electron from the inner shell of the metal atom and as a result electrons from higher energy levels then fill up the vacancy and characteristic X-ray photons are emitted. These X-ray fluorescence photons have distinctive energies, i.e. spectral lines, depending on quantized energy differences of electron orbits of the atom. The operational principle of X-ray tube is described in chapter 7.2.2.

The energy released in transition is not always released as characteristic X-rays. The energy can transfer to an electron of the outer shell which will throw off the atom as Auger electron.

When a charged particle is in accelerating or decelerating motion, part of its kinetic energy transfers to Bremsstrahlung (from the German *bremsen*, to brake and *Strahlung*, radiation). Mainly Bremsstrahlung is generated when the direction of electrons changes in the electric field of nucleus. These Bremsstrahlung photons have continuous energy spectrum. Most of the radiation emitted by the X-ray source is Bremsstrahlung. Figure 1.2 represents the mechanism of X-rays, Auger electron and Bremsstrahlung.

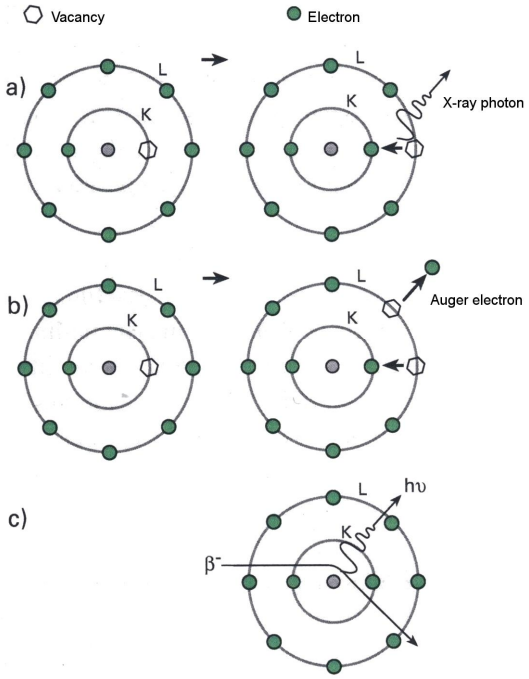

Figure 1.2 The mechanism of (a) X-rays, (b) Auger electron and (c) Bremsstrahlung. [5]

1.3 Gamma rays

Gamma rays are produced by transitions from excited states in a nucleus. Such excited states can be populated in nuclear reactions and in the radioactive decay of the nuclide. When a nucleus emits alpha or beta particle, the daughter nucleus is sometimes left in an excited state. It can then jump down to a lower level by emitting a gamma ray. An example of gamma ray production follows.

First ^{60}Co decays to excited ^{60}Ni by beta decay:

$$^{60}\text{Co} \rightarrow {}^{60}\text{Ni} + e^{-} + \nu_e.$$

The electron (e^-) and the positron (e^+) are also known as β particles, having same physical properties except the opposite charges. Neutrinos (v) are elementary particles that are created as a result of certain types of

radioactive decay or nuclear reactions. There are three types of neutrinos: electron neutrinos (v_e), muon neutrinos (v_μ) and tau neutrinos (v_τ).

Then the ^{60}Ni drops down to the ground state by emitting two gamma (γ) rays in succession:

$$^{60}\text{Ni} \rightarrow {}^{60}\text{Ni} + \gamma.$$

Gamma rays of 1.173 MeV and 1.332 MeV are produced. The decay of ^{60}Co is presented in Figure 1.3.

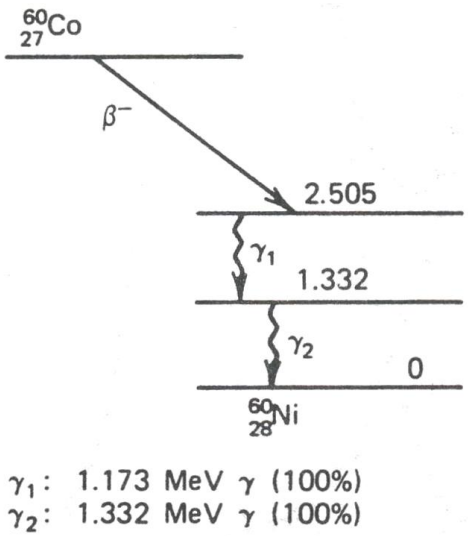

Figure 1.3 Decay of ^{60}Co. [1]

1.4 Radioactive decay

Radioactive decay is a spontaneous process in which an unstable atomic nucleus loses energy by emitting radiation in the form of particles or electromagnetic waves. At the same time the nucleus emits particles or photons. This decay results in an atom of one type, called the parent nuclide transforming to an atom of a different type, called the daughter nuclide. Radioactive decay is a random phenomena and it is not possible to determine in advance when the decay of a specific radioactive nucleus will happen.

However, the quantum mechanical probability for the decay can be determined, proportional to a quantity called half-life ($t_{1/2}$). Half-life is the time taken for the activity of a given amount of a radioactive substance to decay to half of its initial value.

The production of ^{137}Cs, which has a half-life of about 30 years, is illustrated in Figure 1.4. It is dominated by direct fission in mass chain 136 in combination with repeated beta decay. An alternative production path is neutron capture in the stable isotope ^{136}Xe.

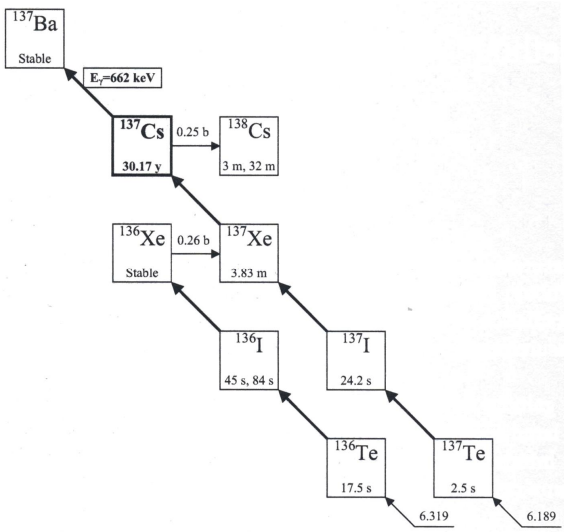

Figure 1.4 Production and decay of ^{137}Cs. Beta decay is illustrated with diagonal arrows and neutron capture with horizontal arrows. [10]

1.5 The fission process

When an unstable heavy nucleus is split into smaller parts, a great amount of energy is released. This process is called the fission reaction and it forms the basis of nuclear energy. In nuclear power reactors neutrons interacting with the fissile nuclei in the fuel cause fission chain reactions and each fission gives rise to approximately 200 mega electron volts (MeV) (1 eV=1.6*10^{-19} J) of energy, two or sometimes three fission products and two or three neutrons. The fission chain reaction is predominantly started by the

absorption of slow neutrons in ^{235}U in the nuclear fuel. It is then self-sustaining since the released neutrons make the fission process continue by splitting the heavy nuclei in the surroundings. An example of a fission reaction is that of ^{235}U:

$$^{235}U+^{1}n\rightarrow^{140}Xe+^{94}Sr+2^{1}n+200\ MeV.$$

Two medium heavy nucleuses are created in the fission process. These nucleuses are called as fission products. Approximately 80 fission products are created directly in fission. While the nuclear reactor is in operation, over 200 different fission products are created via beta decays. The mass number of fission products, that are created in fission, is approximately A=72…160. In Figure 1.5 is presented fission product yield by mass for thermal neutron fission of ^{235}U.

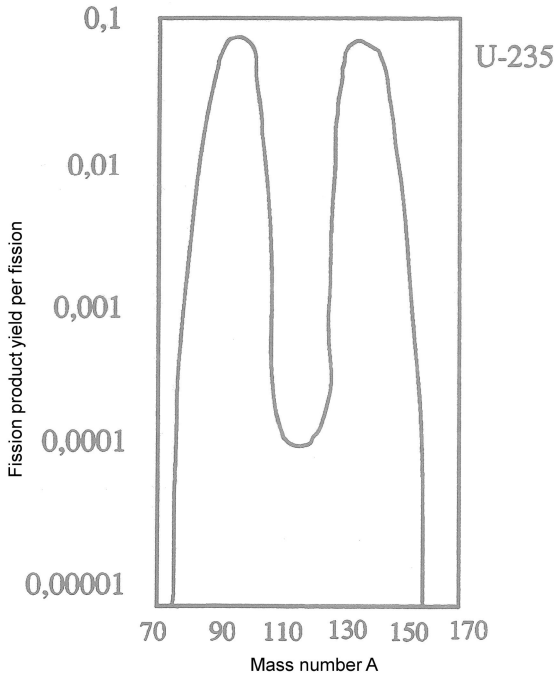

Figure 1.5 Fission product yield by mass for thermal neutron fission of ^{235}U. [21]

The neutrons from the fission are either released directly when the reaction occurs or shortly after and are called prompt and delayed neutrons, respectively. The share of the delayed neutrons is only in the order of a few

percent but they are in spite of this fact crucially important for the control of the fission chain reaction. If all neutrons were prompt the chain reaction would proceed exponentially in a very short time and become impossible to control.

When the neutrons are released they have a relatively high energy, above 100 keV and have to be slowed down. Slow neutrons with energies below 1 eV have a significantly larger inclination to create a fission reaction with a ^{235}U nucleus than fast neutrons. Slow neutrons are also called as thermal neutrons. The probability for a reaction to occur is described as the cross section and is measured in the unit barn [b] (1 barn=10^{-28} m^2). The slowing down of the fast neutrons is taken care of by letting the neutrons collide with particles of approximately the same mass as themselves in the surrounding material. Consequently they will lose energy. The material used in nuclear power reactors for this purpose is called the moderator.

The fission fragments that possess an excess of neutrons are unstable and therefore start decaying immediately which finally leads to various stable nuclei. The fragments are radioactive and decay by emitting particles and/or electromagnetic radiation. Therefore the content of the fuel in a nuclear power reactor changes while the reactor is still operating. The contribution to the fission rate changes from being mainly from ^{235}U in the beginning to depend primarily on new fissile nuclides like ^{239}Pu at the end of the fuel assembly's lifetime. When the fuel has been used to its allowed burnup and is taken out of the nuclear reactor core the decay of the fission fragments continues and radiation is still emitted.

1.6 Nuclear power

A nuclear power plant is built to utilize the released energy in the fission process. When fission occurs, the released energy is transformed mainly into heat. This heat is used to boil or heat water and these mechanisms produces

steam, which is fed to a turbine system, which in turn is connected to a generator that produces electricity. The water used is usually ordinary light water and the reactor type using this kind water is called light water reactor (LWR).

LWR nuclear reactors are mainly two different types, Boiling Water Reactors (BWR) and Pressurized Water Reactors (PWR), where the vast majority of the world's reactors are PWR's. In PWR reactor the heated water is pressurized and is thus prevented from boiling. The steam is instead created in an isolated adjacent system, where the heated water is allowed to interact through heat exchangers producing steam.

In BWR reactor, the heated water is allowed to boil in the reactor core and then fed to the turbines for electric power generation. After the steam has passed turbines, it is condensed and fed back as water into the core and the boiling process is repeated.

Nuclear power produces about 17 % of the electricity produced in the world. At the end of 2007, there were 439 nuclear power reactors operating in the world, with a total net capacity of 372.2 $GW_{(e)}$. Furthermore, there were 33 nuclear power reactors under construction. At the end of 2008, in Finland there were four nuclear power reactors in operation and one is under construction. These four reactors produce about 29 % of the electricity in the country. [3]

2. Interactions of photon with matter

When penetrating matter, photon can interact with the atoms in various ways. The three main interaction processes are photoelectric absorption, Compton scattering and pair production. All these processes lead to the partial or complete transfer of the photon energy to electron energy. They result in sudden and abrupt changes in the photon history, in that the photon either disappears entirely or is scattered through a significant angle. Photoelectric absorption predominates for low-energy photons (up to several hundred keV), pair production predominates for high-energy photons (above 5-10 MeV), and Compton scattering is the most probable process over the range of energies between these two extremes.

2.1 Photoelectric absorption

In the photoelectric absorption process, the photon interacts with one of the bound electrons in an atom, and all of the photon energy is absorbed. The electron is ejected from the atom with a kinetic energy E_e equal to

$$E_e = E_\gamma - E_b \tag{1}$$

where E_γ is the photon energy and E_b the binding energy of the photoelectron in its original shell. This process is shown in Figure 2.1. For typical photon energies, the most probable origin of the photoelectron is the most tightly bound of the K shell of the atom. The vacancy that is created in the electron shell, as a result of the photoelectron emission, is quickly filled by electron rearrangement. This atom will de-excite with the emission of one or more characteristic X-rays or Auger electrons. The Auger electrons have extremely short range because of their low energy. The characteristic X-rays may travel short distance (typically a millimeter or less) before being reabsorbed through

photoelectric interactions with less tightly bound electron shells of the absorber atoms.

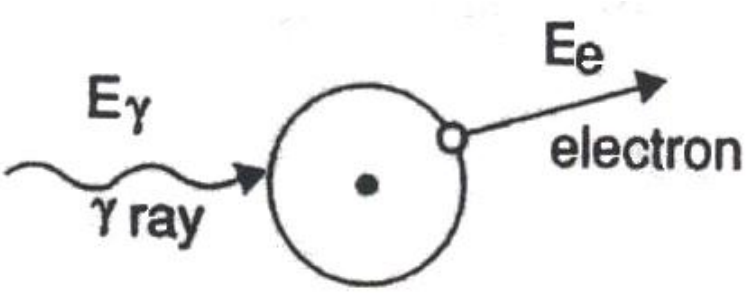

Figure 2.1 The mechanism of photoelectric absorption. [2]

2.2 Compton scattering

Compton scattering is a direct interaction of the gamma- or X-ray with an electron, transferring part of the photon energy. The incoming photon is deflected through an angle θ with respect to its original direction. The photon transfers a portion of its energy to the electron (assumed to be initially at rest), which is then known as a recoil electron. All angles of scattering are possible and the energy transferred to the electron can vary from zero to a large fraction of photon energy. The loss of energy depends on angle of scattering and the original energy of photon. The maximum is gained when the scattering angle is 180° (back scattering). Cross section density of Compton phenomena decrease as a function of energy and it is directly proportional to electron concentration of matter. The mechanism of Compton scattering is shown in Figure 2.2.

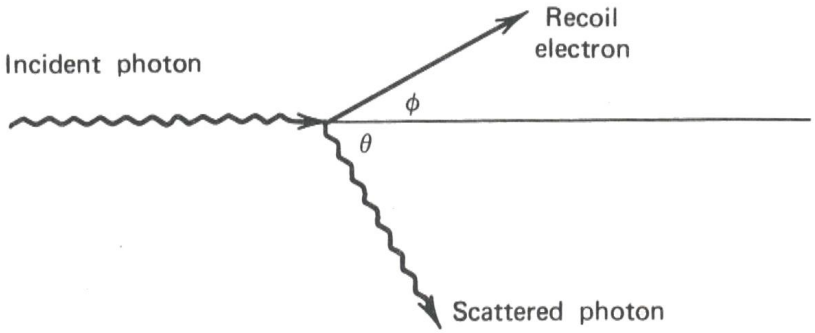

Figure 2.2 The mechanism of Compton scattering. [1]

As a result of Compton phenomena, a scattered photon and a free electron are created. The electron is rapidly absorbed to intermediate agent. The relative meaning of scattered radiation and absorbed radiation can be described with scattering cross-section σ_{cs} and absorption cross-section σ_{ca}.

2.3 Pair production

Pair production results from the interaction of the photon with the atom as a whole. In this process the energy of a photon is converted in nuclear Coulomb field to a positron-electron pair. The photon energy must exceed twice the rest-mass energy of an electron (1.022 MeV). The excess energy is shared between the two particles as kinetic energy. Both the electron and the positron will be slowed down in the intermediate material. The positron will finally react with an electron and annihilate. Two annihilation photons are normally produced as secondary products of the interaction.

The electron and the positron are also known as β particles, having same physical properties except the opposite charges. When a positron has lost enough kinetic energy (mostly all), it combines with an electron and generates annihilation radiation. As a result of pair production the kinetic energies of positron and electron are absorbed to intermediate agent and two 0.511 MeV photons are transmitted to opposite directions. Energy absorption and radiation conversion occurs in pair production. Pair production is most important interaction mechanism in high energies (in lead over 5 MeV and in

tissue or water over 20 MeV). The mechanism of pair production is presented in Figure 2.3.

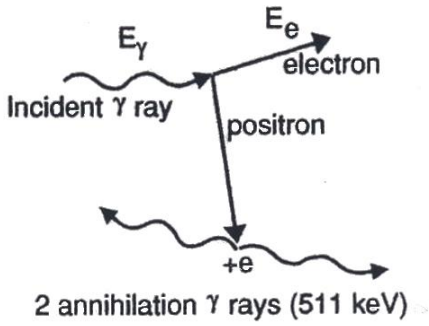

Figure 2.3 The mechanism of pair production. [2]

The relative importance of the three photon-matter interaction processes described above for different gamma- and X-ray energies and absorber materials is illustrated in Figure 2.4. The line at the left represents the energy which photoelectric absorption and Compton scattering are equally probable as a function of the absorber atomic number. The line at the right represents the energy at which Compton scattering and pair production are equally probable.

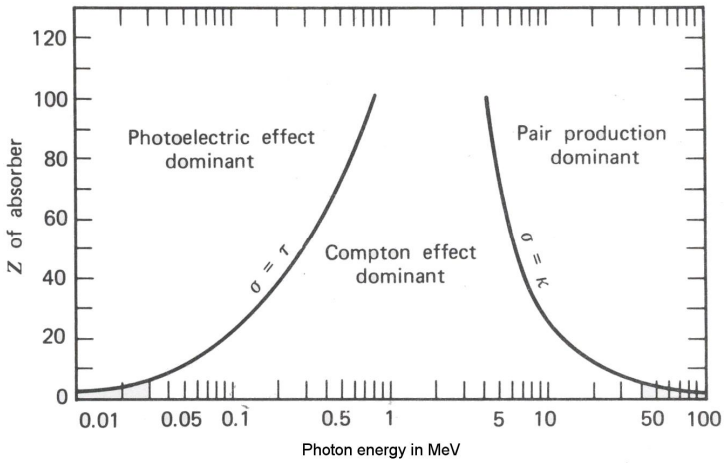

Figure 2.4 The relative importance of the three major types of photon interactions. [1]

2.4 Other interaction processes

There are other photon interaction processes, but they are less probable and less important in the gamma spectrometry and tomography. Two processes, by which the direction of a photon is changed, without loss of energy, are Rayleigh scattering from bound electrons and Thompson scattering from unbound electrons.

3. Semiconductor detectors

3.1 Semiconductors

The electrons of a single atom occupy atomic orbitals, which form a discrete set of energy levels. Combining a collection of atoms together into a solid structure broadens those energy levels into energy bands, each of which contain a fixed number of electrons. The energy of any electron within the pure material must be confined to one of these energy bands, which may be separated by gaps or ranges of forbidden energies. A representation of the electronic bands in insulators, metals (conductor) and semiconductors is shown in Figure 3.1.

The uppermost occupied energy band is known as a valence band by analogy to the valence electrons of individual atoms. In order for an electron to migrate within the material it must be able to move out of its current energy state into another in order to move from atom to atom. If electrons can jump into suitable energy levels then an external electric field applied to the material would cause the current to flow.

In an insulator the valence band is full and the next available energy states are in higher band called the conduction band separated by a forbidden region. In insulators, the electron must first cross the bandgap to reach the conduction band and usually the bandgap is of the order of 10 eV or more.

In a metal the valence bands are not full and in effect the conduction band is continuous with the valence band. Thermal excitation ensures that the conduction band is always populated to some extend and the imposition of a small electric field will cause the current to flow.

In semiconductor, the valence bands are full but the forbidden band gap is much smaller than in insulator, typically 1 eV. For that reason, fewer electrons are found in conduction band and the electrical conductivity is less. Because one of the main mechanisms for electrons to be excited to the conduction band is due to thermal energy, the conductivity of semiconductors is strongly dependent on the thermal temperature of the material. Cooling the material will reduce the number of electrons in the conduction band, thereby reducing the background current (leakage current) and make it much easier to detect the extra excitation due to the gamma-ray interactions. This is the basis of the semiconductor gamma-ray detector.

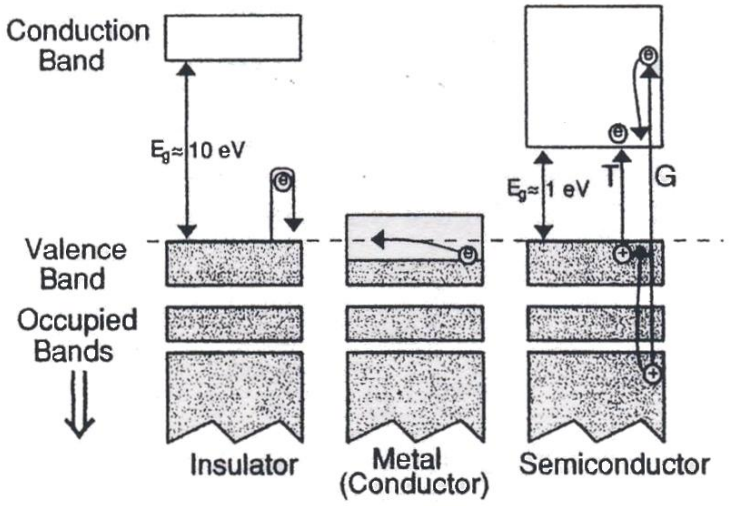

Figure 3.1 Schematic diagram of the electronic band structure in insulators, metals and semiconductors. [2]

3.2 Operational principle of semiconductor detectors

The ideal semiconductor detector material will:

- have as large an absorption coefficient as possible (i.e. high atomic number),
- provide as many electron-hole pairs as possible per unit energy (i.e. low electron-hole creation energy),
- allow good electron-hole mobility,
- be available in high purity as near perfect single crystals,

- be available in reasonable amounts at reasonable cost.

Taking all these qualities into account leaves only a few possible alternatives which are shown in Table 3.1. The best alternative is silicon which is already available at reasonable cost because it is widely used in the field of electronics industry. Its only disadvantage is its low atomic number, which means that in practice it is only used for the measurement of low-energy photons. Detectors based upon silicon are widely used in X-ray spectrometry. Germanium is by far the most common detector material. Its higher atomic number than silicon makes it practicable to use it for the detection of higher energy gamma radiation. High-purity germanium (HPGe) detectors have high energy resolution, which make them suitable for spectrometry purposes.

Table 3.1 Parameters for some materials suitable for gamma-ray detectors. [2]

Material	Atomic number	Operating temperature	Band gap* (eV)	ϵ^* (eV)	Density (g cm^{-3})	Mobility* (cm^2 V^{-1} s^{-1})	
						Electrons	Holes
Si	14	Room temp.	1.106	3.62	2.33	1350	480
Ge	32	Liquid N_2 (77 K)	0.67	2.96	5.32	3.6×10^4	4.2×10^4
CdTe	48, 52	Room temp.	1.47	4.43	6.06	1000	80
HgI_2	80, 53	Room temp.	2.13	4.22	6.30	100	4
GaAs	21, 33	Room temp.	1.45	4.51	5.35		
Bi_2S_3	31, 33		1.3	?	6.73		
PbI_2	82, 53		2.6	7.68	6.16		
GaSe	31, 34		2.03	6.3	4.55		
AlSb	13, 51		1.62	5.05	4.26		
CdSe	48, 34		1.75	?	5.74		

* Band gap, electron–hole creation energies (ϵ) and mobilities are given at 77 K for Ge and 300 K otherwise.

3.3 Configurations of germanium detectors

Germanium detectors are available in a number of different configurations to suit particular applications. The shape of the detector affects its radiation detection efficiency. Respectively, the shape of the detector crystal affects its charge collection capabilities and thus energy resolution.

Planar configuration

A planar HPGe detector is fabricated from high-purity *p*-type germanium. The electrical contacts are provided on the two flat surfaces of a germanium disk. Typically planar detector is used to detect low-energy photons (3-300 keV). In Figure 3.2 is presented a planar HPGe detector

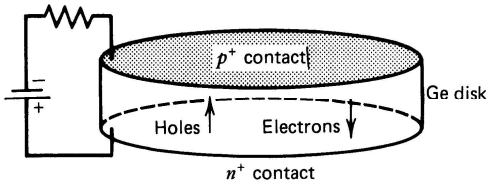

Figure 3.2 Planar HPGe detector. [1]

Coaxial configuration

In coaxial detector the one electrode is fabricated at the outer cylindrical surface of a long germanium crystal. A second cylindrical contact is provided by removing the core of the crystal and placing a contact over the inner cylindrical surface. In Figures 3.3 and 3.4 are presented some properties of coaxial germanium detectors. In Figure 3.5 is presented detector and preamplifier within the cryostat housing.

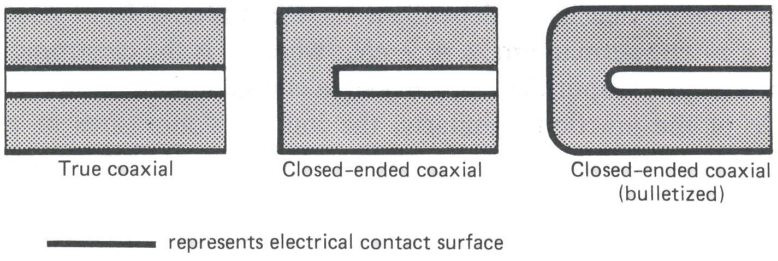

Figure 3.3 Three common shapes of large-volume coaxial detectors. [1]

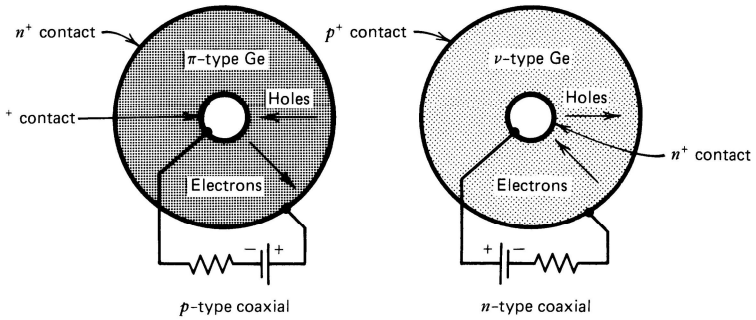

Figure 3.4 Coaxial HPGe detectors. [1]

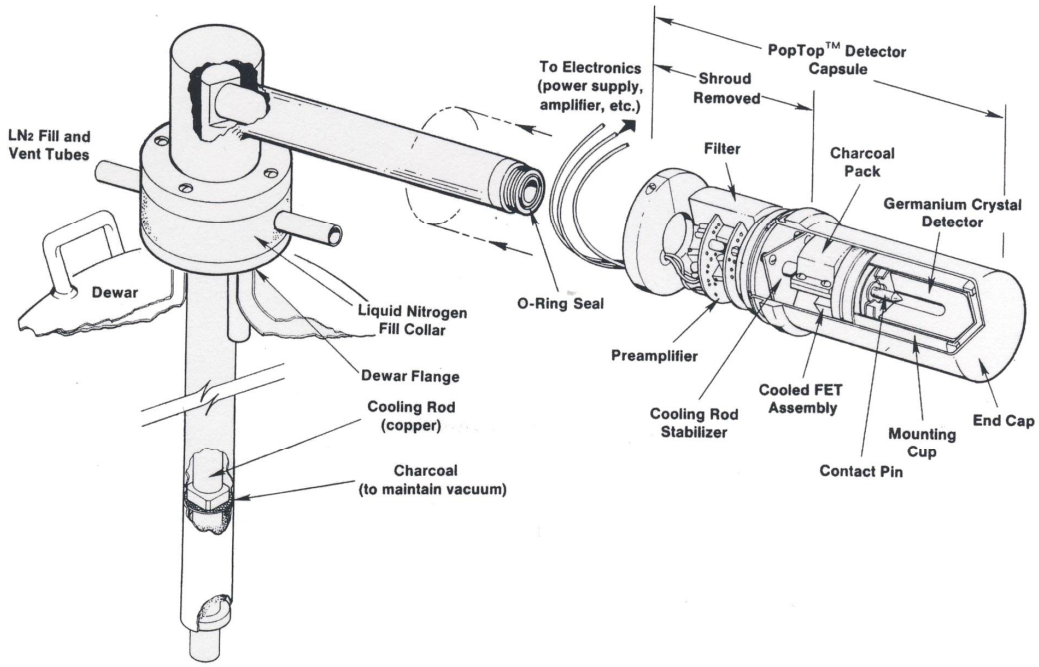

Figure 3.5 Detector and preamplifier within the cryostat housing. (Exploded view of the EG&G ORTEC Pop-Top™ detector capsule with horizontal dipstick cryostat and 20 litre liquid nitrogen container). [2]

Coaxial HPGe detectors are also available in well configurations in which the housing is shaped to allow external access to the hole. Small radioisotope sources can be placed within this well for measurements in which the source is nearly surrounded by germanium detector and the detection efficiency is usually high.

More information about properties of intrinsic, *n*- and *p*-type semiconductors can be found from Ref. [1].

3.4 Other semiconductor detector types

The large majority of semiconductor radiation detectors in current use are manufactured from silicon or germanium. These materials have excellent charge transport properties, which allow the use of large crystals without excessive carrier losses due to trapping and recombination.

Neither silicon nor germanium is ideal from certain standpoints. The other potential semiconductor detector materials have a larger bandgap than germanium and thus would have the advantage of room temperature operation assuming that their other properties were satisfactory.

In gamma-ray spectrometry, detectors with high atomic number are at a premium. Germanium (Z=32) is good alternative, but many other elements would be even better. To date, compound semiconductors have received the most attention as potential room temperature radiation detectors. Some properties of compound semiconductors are presented in Table 3.1.

Cadmium telluride (CdTe) combines relatively high atomic numbers (48 and 52) with large bandgap energy (1.47 eV) to permit room temperature operation. The probability of photoelectric absorption per unit path length is approximately a factor of 4-5 times higher in cadmium telluride than in germanium. CdTe detectors are used in applications where high gamma-ray detection efficiency per unit volume is required.

Cadmium zinc telluride (CdZnTe or CZT) is an alloy of cadmium telluride and zinc telluride. The bandgap varies from approximately 1.4 to 2.2 eV, depending on composition. CZT has several advantages: room temperature operation, very high atomic number and high density leading to good intrinsic detection efficiency. However there are also several disadvantages, the most important being small size. The ternary CZT crystals are limited in size due to physical problems during growth. This small detector size produces a low counting rate compared to other larger detectors and thus requires a longer

counting time for equal statistical precision. The small crystal size also limits the high energy gamma radiation response since higher energy gamma radiation, above 600 keV for example, will have a low interaction probability.

Mercuric iodide (HgI_2) is a semiconducting material with a bandgap width of 2.13 eV. Because of the high photoelectric cross section of mercury (Z=80), low-energy gamma-ray interaction probabilities are as much as a factor of 50 larger than those of germanium. Crystals with a thickness less than 1 mm can show good spectral qualities and have been successively applied in the measurement of X-rays and low-energy gamma rays.

Gallium arsenide (GaAs) is another semiconductor material with a bandgap sufficiently wide (1.45 eV) to permit room temperature operation and it combines relatively high atomic numbers 31 and 33. With respect to germanium and silicon, GaAs has a higher absorption coefficient for X-ray and gamma-ray photons because of its higher atomic number and density. The high electron mobility in GaAs, offers the prospect of high speed particle detection and signal processing. GaAs detectors have good resistance to gamma radiation damage and it is possible to fabricate complex and compact detector geometries (microstrips, pixels, wafers, etc.).

Although several compound semiconductor materials show promise for further development, none of these has reached the point of commercial utilization. Most compound semiconductor detectors are limited to very small sizes and thus their charge collection capabilities can be poor. However, in some applications for example in X-ray radiography, the properties of compound semiconductor detectors are better than HPGe detectors.

3.5 Experimental setup

The conductivity of semiconductors is strongly dependent on the thermal temperature of the material. For that reason, germanium detectors must be cooled to reduce the leakage current to the point that the associated noise does not spoil their excellent energy resolution. The cooling is usually executed with liquid nitrogen and insulated container called dewar. The temperature of liquid nitrogen is about 77 K (-196°C) and the continuous thermal contact between the liquid nitrogen and the detector must be maintained. Cooling can be executed also with electrically operated compressor in which case liquid nitrogen is not needed. In Figure 3.6 is presented common vertical configuration of the detector and liquid nitrogen container.

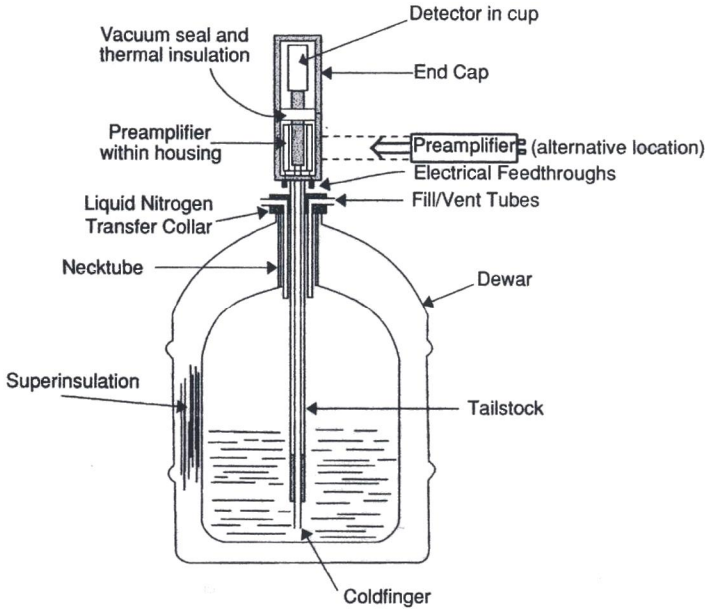

Figure 3.6 Common vertical configuration of the detector and the liquid nitrogen container. [2]

As mentioned before when gamma-rays penetrate into matter, they can interact with the atoms in various ways. The three main interaction processes are photoelectric absorption, Compton scattering and pair production. All

these processes lead to the partial or complete transfer of the gamma-ray photon energy to electron energy.

The output from a gamma-ray detector is an amount of electrical charge proportional to the amount of gamma-ray energy absorbed by the detector. The function of the electronic system is to collect that charge, measure the amount and store the information.

Experimental setup for gamma spectrometry is presented in Figure 3.7. The setup consists of a detector, a preamplifier, a high voltage supply, a detector bias supply, an amplifier and a multichannel analyser. A more comprehensive arrangement might include a pulser, a base line restorer and a pile-up rejector.

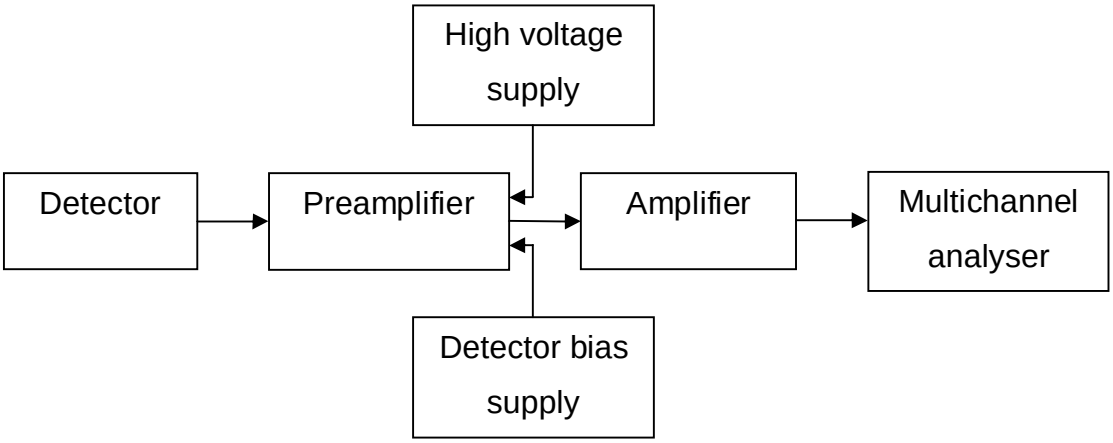

Figure 3.7 A simple schematic electronic system for gamma spectrometry.

3.6 Signal processing

The electrical pulse from a gamma-ray detector is transformed to voltage pulse with a preamplifier and then the voltage pulse is lead to an amplifier where it is shaped and gained. The aim of this operation is to improve resolution of adjacent pulses and to make pulses standard. Adjusting the

shaping time of the amplifier affects to the shape of the pulse. By using long shaping time, one can ensure that all the charges accumulate to the pulse and the energy resolution will be better. In high pulse frequencies, a short shaping time is advised because the risk of coincidence summing will increase otherwise.

From the amplifier the pulses are transferred to pulse height analyzer which is also known as analog-to-digital converter (ADC). The range of energy is divided into channels. Typical amount of channels in gamma spectrometry is 4096 or 8192. The analyzer sorts the pulses by pulse height and counts the number of pulses within individual pulse height intervals.

3.7 Digital signal processing

Today's high performance multichannel analyzer systems are designed using digital signal processing (DSP) techniques rather than the traditional analog methods. DSP filters and processes the signals using high speed digital calculations rather than manipulation of the time varying voltage signals in the analog domain.

4. Nuclear fuel

The nuclei ^{233}U, ^{235}U, ^{239}Pu and ^{241}Pu are called fissile nuclei since they easily fission when hit by a neutron with relatively small kinetic energy. ^{239}Pu and ^{241}Pu are produced in nuclear reactors while ^{235}U exist in nature but with small abundances. ^{233}U does no exist in nature and it is derived in nuclear reactor from ^{233}Th. ^{235}U is derived from the nature existing uranium ores and can be used as fuel in nuclear power reactors.

Natural uranium consists to 99.3 % of ^{238}U and 0.7 % of ^{235}U. Before the uranium can be used as fuel in the light water reactors it has to be enriched, i.e. the fraction of the fissile isotope ^{235}U must be increased to typically 3-5 % [4]. After the enrichment the uranium is converted to uranium dioxide (UO_2) powder which is sintered into small cylindrical pellets with a length and diameter of about one centimetre. The pellets are stacked into about four meter long cladding tubes made out of zircaloy, making up a fuel rod. Zircaloy has good corrosion durability, endures high temperatures well and has a small neutron capture cross section, making it suitable for use in nuclear reactors. Finally the fuel rods are typically arranged in quadratic or hexagonal lattices called fuel assemblies of different sizes depending on the type of reactor they are used in. In Figures 4.1 and 4.2 are presented the fuel elements of PWR and BWR. In Figure 4.3 is presented a cross-section of a PWR fuel rod.

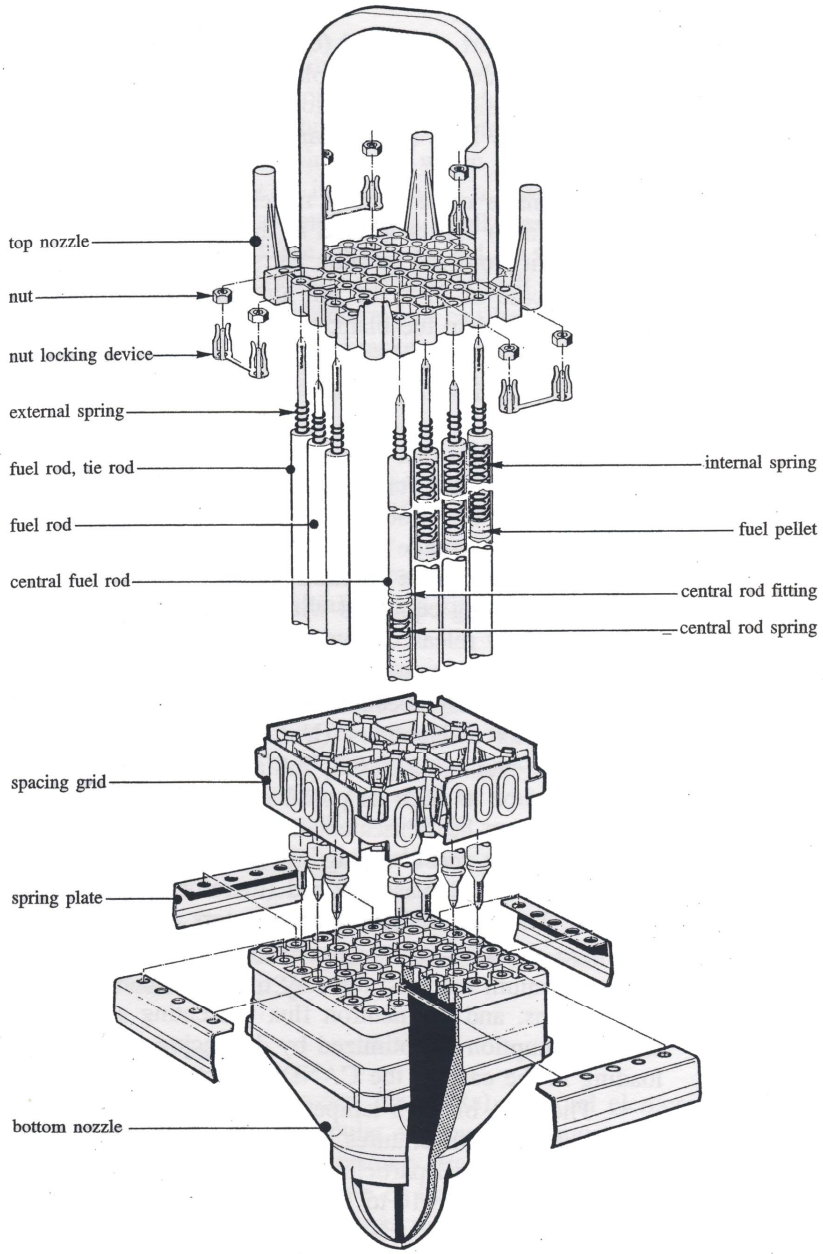

Figure 4.1 BWR fuel element. [4]

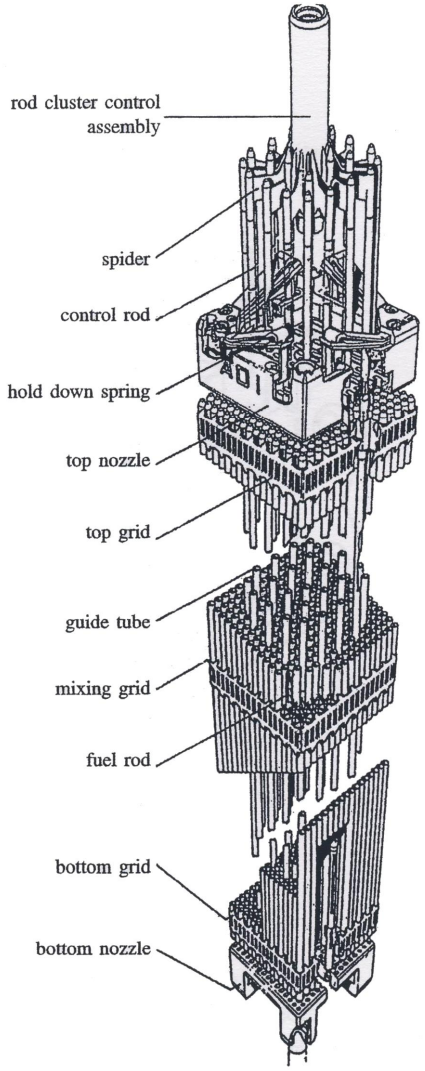

	900 MW	1300 MW
number of rods	264	264
number of grids	8	10
length	4.00 m	4.80 m
cross-section	21.4 x 21.4 cm	
total weight	670 kg	765 kg
uranium weight	461 kg	538 kg
number of assemblies	157	193

Figure 4.2 PWR fuel element and control rod cluster. [4]

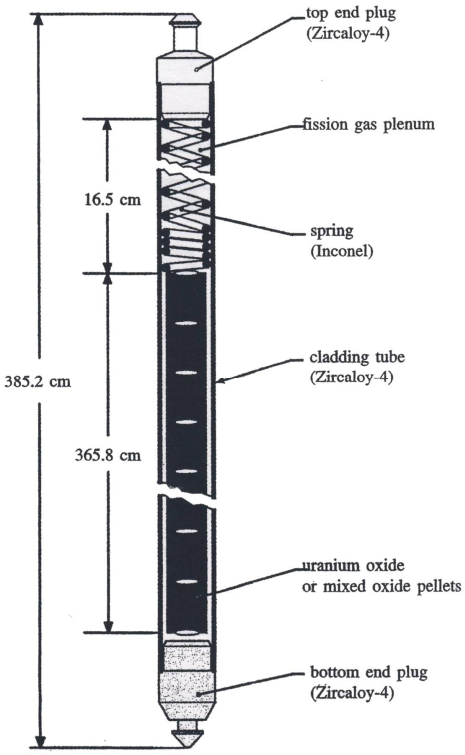

Figure 4.3 Cross-section of a 900 MW_e PWR fuel rod (the dimensions in cm are nominal). [4]

The uranium dioxide has the qualities desirable for nuclear fuel: namely a high melting point, endurance to radiation damage and it is chemically inert [7]. The main disadvantage of UO_2 as fuel material is its low thermal conductivity. However this drawback is partially offset by the fact that very high operating temperatures are possible in the centre of the fuel rod due to the high melting point [6]. The most important physical properties of UO_2 are summarized in Table 4.1.

Table 4.1 Physical properties of uranium dioxide (UO_2).

Property	**Value**
Melting point	2865°C (5189°F)
Theoretical density	10.97 g/m^3
(without any porosity present in the material)	
Thermal conductivity	4.777*10^{-3} W/m*K at 20°C
	1.91*10^{-3} W/m*K at 1000°C
Thermal expansion coefficient (per °C)	~1*10^{-5}/°C (0 to 1000°C)
Tensile strength	6.9*10^{7} Pa (10 000 psi)
Coefficient of elasticity	1.72*10^{11} Pa (25*10^{6} psi)
Thermal expansion coefficient	~10^{-5} (0 to 1500 °C)
Specific heat	63.6 $Jmol^{-1}K^{-1}$ (25 °C)
Fracture strength	~110 MPa
Modulus of elasticity	2.0 (at 20 °C)

4.1 Parameters of irradiated nuclear fuel

Burnup

This quantity describes the total energy produced in the fuel. It is measured in unit GWd/tU which is gigawatt days of thermal energy produced per tonne uranium present in the fuel.

Cooling time

The time passed since the reactor shutdown i.e. the time passed since the reactor was subcritical.

Decay heat

The heat of spent nuclear fuel assembly. The decay heat is produced from mainly decaying fission fragments.

Initial enrichment

The amount of ^{235}U present in the fuel i.e. prior to irradiation.

Irradiation history

A detailed description how the burnup is distributed in time.

4.2 Operational properties of nuclear fuel

While in the reactor, the fuel undergoes numerous transformations. Various physical, mechanical and physicochemical reactions are linked to high temperature and steep radial temperature gradient within the pellets. For PWRs, a typical temperature of the fuel is of the order of 500 °C to 1000 °C [4]. This causes modifications in the fuel structure. Following reactions are the most important in the field of gamma spectrometry and tomography of nuclear fuel.

Fuel swelling and densification

During irradiation the volume of UO_2 fuel changes continuously with burnup. Initially, at the start of irradiation, there is a contraction in volume as pores remaining from sintering process continue to shrink. This process is most pronounced in low-density fuel and especially if the pores are small, typically less than 1 μm in diameter. The pellet-cladding gap thus increases at the beginning of the irradiation due to the fuel densification, giving higher fuel temperatures. [16]

The process of fuel densification quickly saturates and is followed by an increase in volume as more and more fission products replace the fissionable uranium. This can result in both radial expansion and elongation of the fuel

pellets and can in severe cases during high power transients even cause a fuel failure.

Fission gas release

A majority of the fission products created at the time of fission are unstable short-lived nuclides. Given the in-reactor irradiation time of the fuels, it is primarily the fission products having half lives longer than a few days which significantly influence the behaviour of the fuel [4]. Those having half lives exceeding several years are considered to be metastable on the irradiation time-scale.

Fission products remain within the fuel and produce several effects: swelling and modification of the physical and physicochemical properties of fuel, or these fission products can be released, creating a gaseous pressure within the cladding. They can deposit themselves on the cladding, causing corrosion. The swelling is caused by a number of mechanisms:

- solid fission products,
- fission gas as individual atoms,
- fission gas precipitated into intra-granular bubbles,
- fission gas as grain boundary bubbles (inter-granular).

The first two are classified to as inexorable swelling since the volume change they cause is only dependent on burnup. They are hard to separate experimentally and thus are referred to as solid fission product fuel swelling. Sufficiently high temperature is required to permit atomic migration and to cause a swelling by formation of gas bubbles. The largest single contribution to fuel swelling originates from inter-granular fission gas bubbles. Microscopy on cross sections of fuel rods operated at high temperatures reveals the presence of cigar shaped pores at the grain boundaries. Examination of fractured surfaces of irradiated fuel show gas bubbles on grain surfaces and also along grain edges. Measurement of the change in volume after

isothermal irradiation of both restrained and unrestrained UO_2 samples shows that the swelling rate is strongly dependent on fuel temperature. [16]

The fuel lattice swelling consists of fission gas bubble swelling (which is strongly temperature dependent) and solid fission product swelling (which is essentially temperature independent). The solid fission products causing swelling can be divided into three groups, soluble fission products (Nb, Y, Zr), metallic inclusions (Mo, Ru, Te, Rh, Pd) and others (Cs, Rb, I, Ba, Sr). When isolated in the UO_2-lattice, the rare gases Xe and Kr should be added, when evaluating the contributions to the solid swelling.

The gaseous fission products are primarily rare gases:

- xenon in the isotopic forms ^{129}Xe, ^{131}Xe, ^{132}Xe, ^{134}Xe and ^{136} Xe,
- krypton ^{83}Kr, ^{84}Kr, ^{85}Kr and ^{86}Kr,
- helium created by a few ternary fissions, neutron capture by oxygen and the alpha decay of some isotopes such as ^{238}Pu, ^{241}Am or ^{242}Cm.

Two main processes occur in fission gas release (FGR). The first is the basically temperature independent athermal release and the second is thermal release through a diffusion mechanism which gives a rise to temperature dependency.

In athermal release two distinct mechanism are involved. Direct recoil release is possible if a fission event is taken place close enough (~8 μm) to a free surface. Due to its high kinetic energy, in the range of 60-100 MeV, the fission product will escape the fuel. Usually these atoms are trapped in the cladding but some will be stopped in the gap through the UO_2 leading to a high local heat pulse along its path. When the fission product leaves or enters a free fuel surface, the heated local zone will evaporate or sputter. This second mechanism is referred as knockout.

Thermal fission gas release is a temperature dependent release mechanism with onset above ~700 °C [17]. It includes lattice diffusion of gas atoms to

grain boundaries, trapping of gas atoms by crystal defects or gas bubbles, fission induced re-solution of grain boundary bubbles and saturation of grain boundaries with gas bubbles leading to macroscopic release. When the temperature is high enough, bubbles will nucleate, grow and interlink leading gas to escape to the rod free volume.

Fuel microstructure

The radial variation in the fuel pellet microstructure (pores and gas bubble size, grain size and fission product disposition) is a good indicator of the status and in-pile behaviour of the fuel and has dependence to the possible fission product release during a transient. At high burnup, especially the edges of the pellet undergoes significant micro-structural changes associated with the enhanced local burnup caused by resonance neutron capture in ^{238}U and the resulting plutonium buildup and fission [15]. Above a local burnup threshold (~70 MWd/kgU) significant microstructural changes are observed like lower dislocation density and lower density of intragranular bubbles.

Volatile element migration

Volatile elements are particularly sensitive to migration, i.e. relocation of elements in the fuel matrix due to high temperatures. Xenon, cesium and iodine are examples of volatile elements encountered in the nuclear fuel matrix. The behaviour of xenon has been discussed earlier. Cesium and iodine are in the gaseous state at temperatures present in the fuel pellet. They will therefore undergo considerable radial and axial migrations and, in some cases, are likely to accumulate when coming into contact with the cladding, causing it to corrode.

5. Gamma spectrometry of nuclear fuel

In gamma spectrometry of nuclear fuel the gamma-ray flux emitted from unstable isotopes is measured using high-resolution gamma-ray spectroscopy [2]. The production of unstable isotopes correlates in with various physical fuel parameters. In Table 5.1 are presented the main isotopes that may be used in gamma-ray measurements of nuclear fuel.

Table 5.1 Main gamma emitter radionuclides present in an irradiated fuel spectrum according to their half-life. Noble gases are marked with red color, volatile elements are marked with blue color and semi or non-volatile elements are marked with green color.

Short half-life		**Middle half-life**		**Long half-life**	
Measurable from 1 hour to 1 day		**Measurable from 1 day to some weeks**		**Measurable from 1 month to some years**	
Fission product	**Half-life**	**Fission product**	**Half-life**	**Fission product**	**Half-life**
^{88}Kr	2.8 h	^{95}Zr/^{95}Nb	64 d/35 d	^{85}Kr	10.7 y
^{91}Sr/^{91m}Y	9.5 h/ 0.8 h	^{99}Mo	2.8 d	^{95}Zr/^{95}Nb	64 d/35 d
^{92}Sr/^{92}Y	2.7 h/ 3.7 h	^{103}Ru	39 d	^{103}Ru	39 d
^{93}Y	10.5 h	^{127}Sb	3.8 d	^{106}Ru	1.0 y
^{97}Zr/^{97}Nb	17 h/1.2 h	^{131}I	8.0 d	^{125}Sb	2.8 y
^{105}Ru/^{105}Rh	4.4 h/ 35.5 h	^{132}Te/^{132}I	3.2 d/ 2.3 h	^{134}Cs	2.1 y
^{133}I	20.8 h	^{133}Xe	5.2 d	^{137}Cs	30.1 y
^{134}I	0.9 h	^{133m}Xe	2.2 d	^{141}Ce	32 d
^{135}I	6.6 h	^{140}Ba/^{140}La	12.8 d/ 1.7 d	^{144}Ce	284 d
^{135}Xe	9.1 h	^{141}Ce	32 d	^{154}Eu	8.6 y
^{143}Ce	1.4 d	^{143}Ce	1.4 d		
		^{147}Nd	11.1 d		
		^{239}Np	2.43 d		

Measurements can be executed in several ways.

Lengthwise measurements on fuel samples:

- Power and burn-up profiles (long life radionuclides),

- Nuclide identification (qualitative measurement)
- Profile evolution of fission products, activation products and heavy nuclides,
- Geometrical characteristics of the fuel column,
- Fission products profiles (short & long life radionuclides),
- Fuel shifting,
- Migration of volatile fission products along the rod,
- Fission gas release (^{85}Kr measure in the fission gas plenum).

Radial measurements on fuel samples:

- Geometrical characteristics e.g. fuel column diameter,
- Gradients.

Other quantitative measurements:

- Flux profile measurement,
- Dosimetry pin measurement,
- Linear activity, fission density, burn-up,
- Measurements for gamma scanning calibration,
- Multiscanning for tomography reconstruction.

Other uses:

- Periodic controls for operation,
- Dismantling.

5.1 Measuring methods

Lengthwise measurements

During a lengthwise examination, the fuel element or rod is moved parallel to its axis perpendicularly to the collimation slit. Several hundred successive and joined spectra help to explore the entire length of the fuel element or rod.

The spatial resolution is linked to the width of the collimator slit. The main applications of this type of measurement are: dimensional measurements of the fissile column, determination of longitudinal migration of fission products, determination of burnup and/or irradiation power, quantitative distribution of fission products or global balance on the fuel element or rod.

Burnup comparison between fuel rods is obtained using ^{137}Cs activity from the fuel column measured at a reference position, usually 2000 mm from the bottom of the approximately 4 m long fuel pellet column. The ^{137}Cs intensity is proportional to burnup. Cesium migration may interfere with burnup determination, but, if checked to be significant, measurements covering at least a full pellet length will be reliable.

Fission gas release is determined by high-resolution gamma-ray spectroscopy of the plenum content of ^{85}Kr [17]. ^{85}Kr is measured after the fuel rod has been stored for 0.6-2 years, allowing short-lived nuclides such as ^{58}Co to decay. ^{85}Kr is the only fission gas product with a sufficiently long half-life (10.7 y) for this purpose. The decay of ^{85}Kr is accompanied by the emission of a 514 keV photon in only 0.2% of the disintegrations, and the fission yield is also relatively low. A problem is to separate the 514 keV peak from the 511 keV annihilation radiation and from 512 keV photons due to the decay of ^{106}Rh. Cobalt impurities in the plenum spring of standard LWR fuel give rise to a strong ^{60}Co gamma source whose Compton distribution tends to overshadow the 514 keV ^{85}Kr peak. A Compton suppression system can be used to avoid this problem.

^{140}La, whose efficient decay rate is controlled by the mother nuclide ^{140}Ba with a half-life of 12.7 days, reflects an average axial power distribution that is representative of the latest weeks of operation of the reactor. A feasible opportunity to measure ^{140}La is within 2-3 weeks after irradiation when the decay chain ^{140}Ba→^{140}La→^{140}Ce has reached secular equilibrium and the decay of ^{140}La is effectively governed by the half-life of ^{140}Ba. Another aspect of relevance is the fact that the 1596 keV gamma ray peak of ^{140}La is the

dominant feature in the gamma ray energy spectrum after around two weeks of cooling time.

Transversal examination

For this type of examination the fuel element or rod is moved perpendicularly to its axis and parallel to the collimation slit. All of the joint spectrums acquired are called a “projection”. The exploitation of this projection, as in the lengthwise measurements, provides access to the geometric characteristics and especially the fuel diameter. The main applications of this type of measurement are: spatial distribution of fission products and determination of flux or power depletion of the measured fuel element or rod.

5.2 Detector types

A high-purity Ge p-type detector (HPGe) is used for measurements where good energy resolution is needed (fission gas release, burnup and power distribution).

For the axial gamma scanning of cesium redistribution a sodium iodide (NaI) scintillator detector is usually used because cesium is the dominating activity.

The energy resolution cadmium-zinc-telluride (CZT) detectors has been improved, to such extent, that they can replace the more difficult to use HPGe detectors in certain spent fuel gamma measurements. This allows the design of a compact underwater partial defect verification device for LWR spent fuel assemblies.

Bismuth germanate (BGO) detector have high scintillation efficiency, good energy resolution between 5-20 MeV and it is mechanically strong. Typically BGO detector is used in Compton suppression spectrometer.

5.3 Mechanical arrangement

The first gamma spectrometry experimental devices on irradiated nuclear fuel appeared in the 1960s with the installation of a measurement bench in a high activity cell. Then, quickly so called “immersed benches” have been built. The aim of this technique is to use it in a quantitative way to obtain the physical parameters of irradiation or to interpret experiments.

Nowadays gamma spectrometry measurements of irradiated nuclear fuel are performed either in high activity cell (hot-cell) or in a pool filled with water (reactor pool, fuel storage pool, etc.). In both cases mechanical arrangement includes following components:

- mechanical bench or fixture,
- collimator(s),
- detector (and cooling system),
- detector shielding (can be part of the collimator),
- data processing system.

In a water filled pool case the gamma spectrometry measurements of irradiated nuclear fuel can be performed with two different methods. Both detector and small collimator in a watertight container is submersed to pool and moved around fuel assembly or fuel assembly is moved in front of the collimator which is positioned a few meters below water-level.

Fuel assembly is positioned into a mechanical bench or fixture that can be elevated and rotated relative to a horizontal collimator slit mounted in the pool wall. Typically the fuel assembly can be positioned laterally and angularly within a few millimeters and one degree. In Figures 5.1 and 5.2 is presented the mechanical arrangement for gamma spectrometry measurements of nuclear fuel.

The collimator component is presented in Figures 5.3 and 5.4. The upper follow-through is used for gamma emission measurements and the lower follow-through for X-ray transmission measurements. There is variety of collimation slits in the pre-collimator. The pre-collimator can be rotated so that suitable collimation slit can be chosen. There is a possibility that photons scattered from other collimation slits can reach the detector. For that reason the distance between two collimation slits have to be at least 7 centimeters so that unwanted radiation from other collimation slits is reduced to acceptable level. [9]

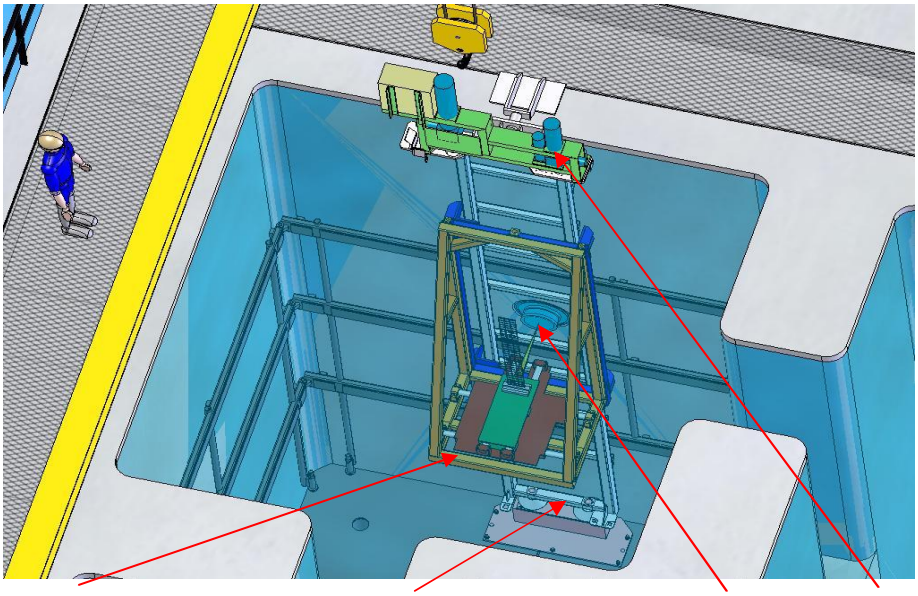

Figure 5.1 Gamma spectrometry system in the storage pool. [18]

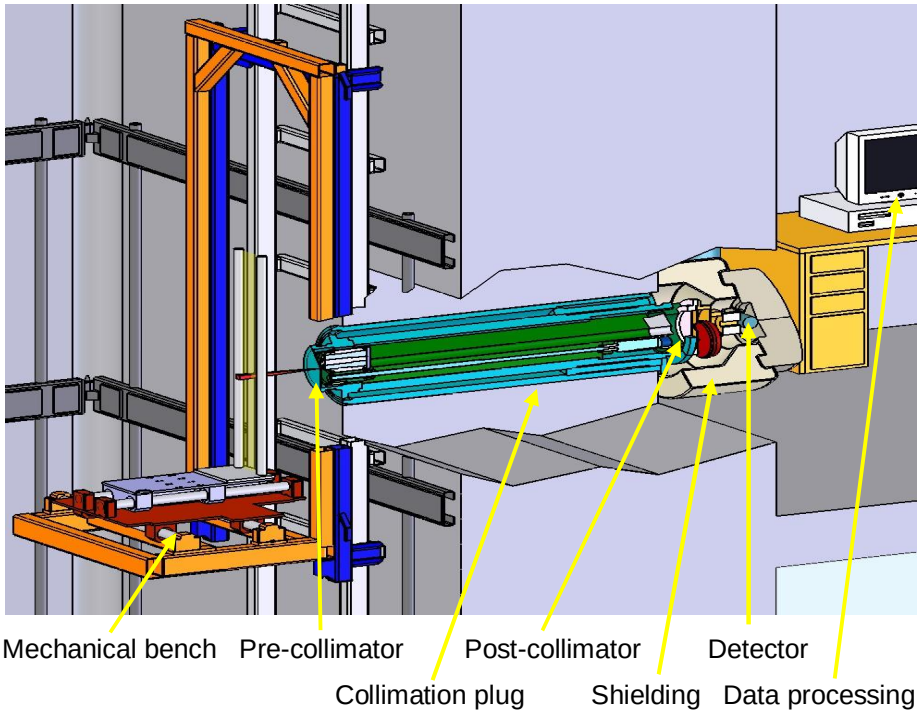

Figure 5.2 Cutaway of a standard gamma spectrometry system. [18]

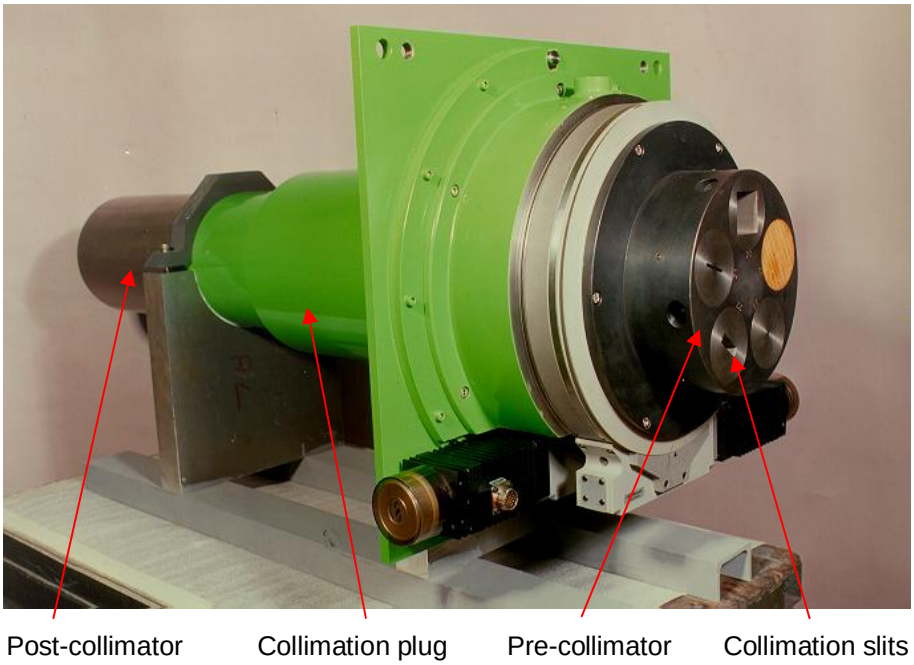

Figure 5.3 View of a collimation plug component. [18]

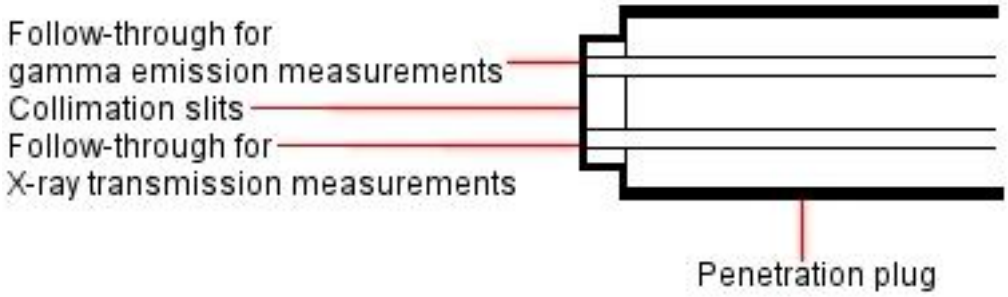

Figure 5.4 Follow-throughs of collimation plug component.

5.4 Advantages and disadvantages

Gamma spectrometry has been applied to solid, liquid and gaseous samples with a low activity and these are measured on simple geometrical supports for a number of years in different laboratories. Properties of irradiated nuclear fuel and the type of its gamma emitters require a more complex implementation, both for the acquisition of spectra and their analysis and interpretation.

High activity

The first limiting physical parameter for gamma spectrometry measurements of nuclear fuel is the very high activity of irradiated fuel: typically of about 10^{12} Bq per 1 cm fuel rod section. This parameter affects the acquisition geometry: distance between the emission source and the detector has to be optimized and aperture collimator limiting the gamma ray beam between the emission (fuel) and the reception (detector) is needed. This equipment is needed to prevent saturation of the detector and to block unwanted radiation from the detector.

Absorption of gamma radiation

The second parameter affecting the quantitative measurements is the intrinsic characteristics which the fuel is analyzed. The fuel is “seen” through

different structures (mechanical parts of the fuel element or fuel rod) which must taken into account to go from the measurement of the spectrum to the corresponding activity of these radionuclides contained in the fuel section analyzed, or to their concentration in number of atoms per length unit examined.

Complexity of spectrum coming from the measurements of irradiated fuel

Another aspect which provides all its difficulties to this type of spectrometry and represents the great difficulty in using spectrum on irradiated fuel is the significant complexity of the spectrum coming from the measurements. There is high number of gamma rays to identify and there are interferences between gamma rays (gamma rays overlapping each other, which must be deconvoluted). In Figure 5.5 is presented an example of spectrum complexity on freshly irradiated fuel (red) and comparison with the same fuel sample cooled for several years (blue). Over 40 nuclides can be identified somehow between 500 keV and 800 keV.

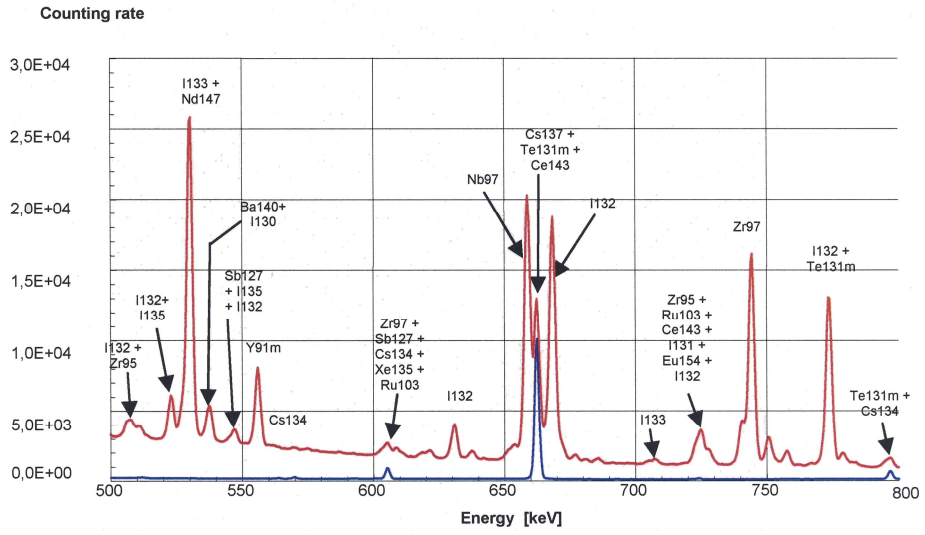

Figure 5.5 Example of spectrum complexity on freshly irradiated fuel (red) and comparison with the same fuel sample cooled for several years (blue). [18]

Accuracy of mechanical bench

The fuel assembly should be able to be positioned laterally and angularly with accuracy within a few millimeters and one degree. Typically the mechanical bench is submersed either reactor pool or fuel storage pool. When the reactor is in operation it produces a great amount of heat which conducts to the water. This causes a circulation of water. Circular motion of water causes the mechanical bench to move and this unwanted movement has to be muted someway.

6. Tomography

6.1 Principle

Tomography means techniques to create sectional images of the interior of objects by performing external measurements. The method is used in the field of non-destructive testing (NDT), medicine, archaeology, biology, geophysics and other sciences [20]. In most cases it is based in the mathematical procedure called tomographic reconstruction.

Several methods are available, delivering specific images, depending on the selected physical excitation:

- Nucleonic methods
  - transmission (photon transmission and neutron transmission)
  - emission (SPECT (Single Photon Emission Computed Tomography) and PET (Photon Emission Tomography))
  - scattering (neutron scattering and gamma ray scattering),
- Optical methods
  - transmission
  - emission (infra-red)
  - interferometry
- Microwave and NMR (Nuclear Magnetic Resonance) methods
  - microwave diffraction
  - NMR
- Acoustic methods
  - transmission
  - reflection
  - TOF (Time-of-flight)
  - diffraction
- Electrical methods
  - capacitance

- resistance.

In this thesis the emphasis is in techniques which are used in tomography of nuclear fuel. These techniques are: gamma emission tomography and X-ray transmission tomography.

6.1.1 X-ray transmission tomography

In X-ray transmission tomography the photons are detected after transmitted through the investigated object as in Figure 6.1. It is based on the application of equation, known as the Beer-Lambert law, or attenuation law.

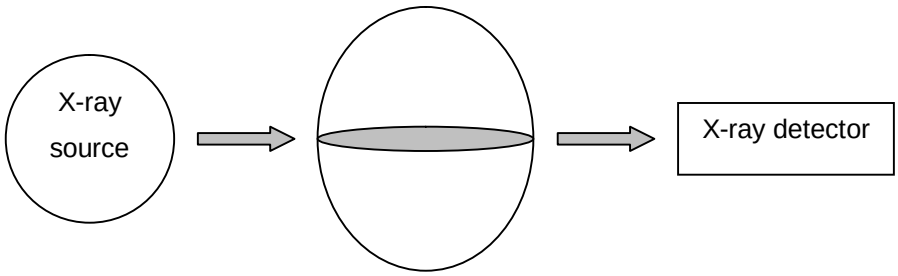

Figure 6.1 X-ray transmission tomography.

This thesis will be focused on transmission tomography which is widely used in both industrial and medical fields. It is based on the application of equation (2), known as the Beer-Lambert law, or attenuation law. In Figure 6.2 is presented the example of Beer-Lambert absorption. Figure 6.5 describes the basic experimental set-up for transmission tomography inside a single slice.

Introduction of Beer-Lambert law follows.

$$A=\varepsilon bc \tag{2}$$

where

A=absorbance of the sample

ε=absorption coefficient

b=thickness of the sample

c=concentration of absorbing species in the material

$$T = \frac{T_1}{T_0} = 10^{-\varepsilon bc} \tag{3}$$

$$\int_{I_0}^{I_1} \frac{dI}{I} = -\int_0^b kc\, dx$$

$$\ln \frac{I}{I_0} = \frac{\log \frac{I}{I_0}}{\log e} = -kbc \leftrightarrow A = -\log \frac{I}{I_0} = \log ekbc = \varepsilon bc \rightarrow A = \varepsilon bc$$

$$I = I_0 \int_L \mu(E)\, dl \tag{4}$$

where

T=transmittance

I=radiation intensity

l=thickness of each material

μ(*E*)=lineic attenuation.

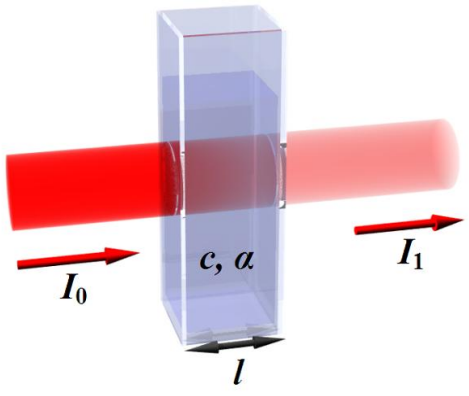

Figure 6.2 Diagram of Beer-Lambert absorption of a beam of light as it travels through an object. [19]

6.1.2 Scattered photons tomography

Scattered photons tomography is based on the clear differentiation between Compton and Rayleigh scattered photons as shown in Figure 6.3.

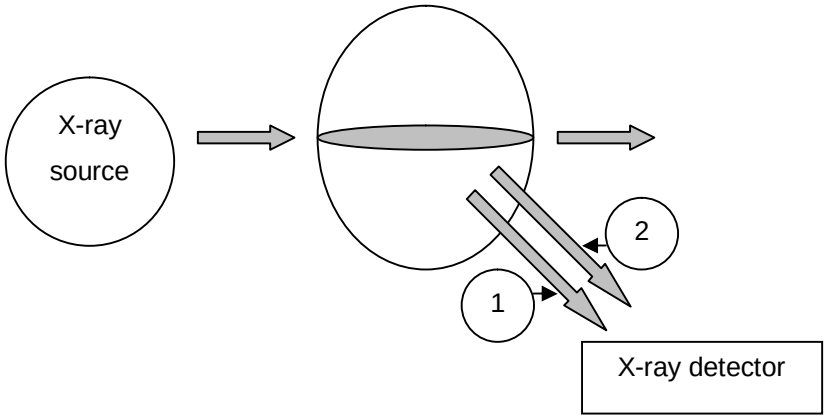

Figure 6.3 Scattered photons tomography. 1. Rayleigh scattering. 2. Compton scattering.

6.1.3 Emission tomography

In emission tomography the photons emitted by the investigated object itself are detected as shown in Figure 6.4. In this case gamma-ray sources are distributed inside the object to be measured or the source itself emits gamma radiation.

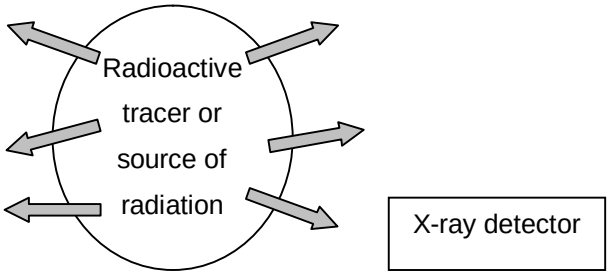

Figure 6.4 Emission tomography.

6.2 Principles of computed tomography

The principle of computed tomography consists of measuring the spatial distribution of a physical quantity to be examined from different directions and to compute superposition-free images from these data [20]. For survey radiographs, the relative distribution of the X-ray intensity is recorded, i.e. for classical radiographs, only the gray value pattern is utilized to derive a diagnosis. In computed tomography, the intensity of X-rays is also recorded behind the object. In addition to the intensity I attenuated by the object, the primary intensity I_0 has to be known in computed tomography to calculate the attenuation value along each ray from source to detector.

To be able to compute an image in acceptable quality following Radon's theory [8], a sufficiently high number of attenuation integrals or projection values have to be recorded. It is necessary to carry out measurements from many directions: image reconstruction algorithms may require projection data over the entire angular range of 360°, with many narrowly spaced data points for each projection.

A simple measurement setup is presented in Figure 6.5. A radiation source with adequate collimation emits a pencil beam and the intensity, attenuated by the object, is registered by the detector placed opposite. For a given angular position, this setup of a radiation source and detector is moved linearly (translation), and the intensity is measured either at single discrete points or continuously. This result in an intensity profile recorded for parallel rays. By determining the ratios of the primary intensity recorded in the periphery and attenuated intensities recorded behind the object and taking their logarithms, an attenuation profile results, which is generally termed a projection. Projections are measured successively for successive angular positions. The complete set of projections is then transferred to the data processing unit, where the image is reconstructed.

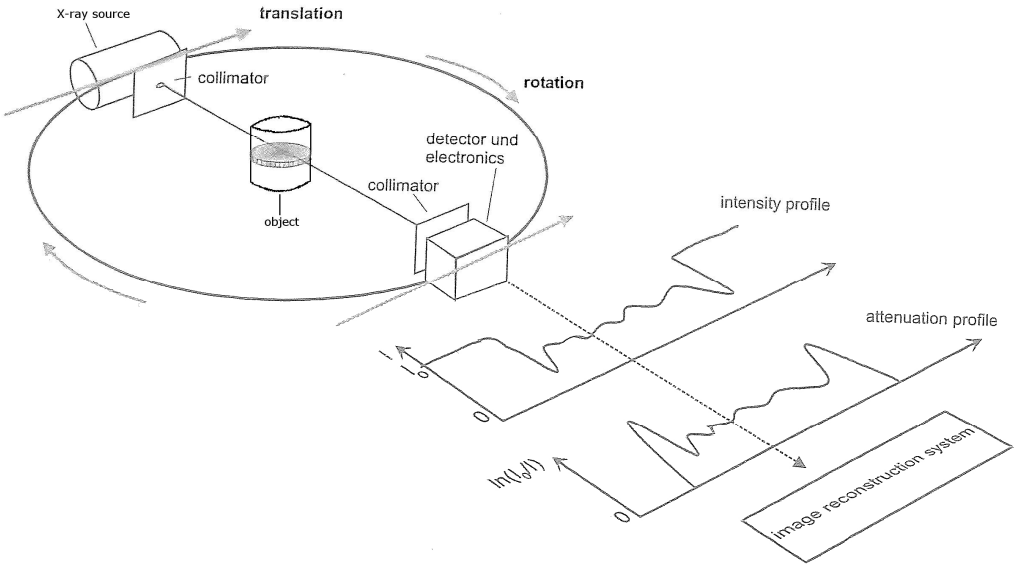

Figure 6.5 Simple measurement system for computed tomography.

6.3 Radiography and 2D- and 3D-tomography

In radiography measurements the X-ray source and detectors move synchronously along vertical axis. Position of the object is fixed. As a result is a digital radiography image. In Figure 6.6 is presented the principle of radiography imaging.

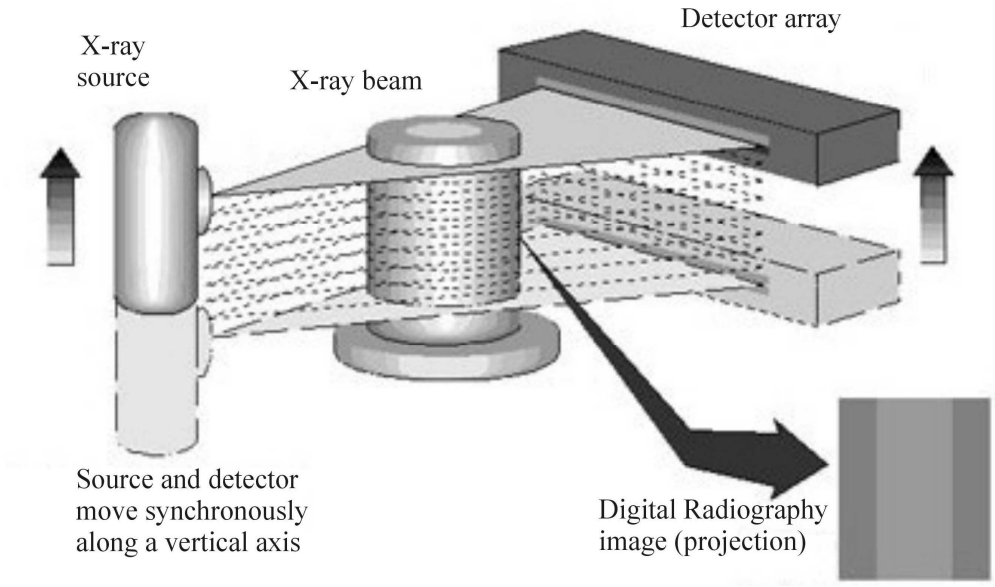

Figure 6.6 The principle of radiography imaging. [14]

In 2D-tomography the positions of the X-ray source and detectors are fixed and the object rotates around its axis. When a sufficient number of projections is recorded from different angles, mathematical image reconstruction algorithms can be used to generate a 2D density map of the object, a 2D cross section image.

In 3D-tomography measurements, the object is in addition moved axially, either stepwise or with simultaneous rotation around the axis, leading to helical trajectory for each projection measurement. Again, applying suitable image reconstruction algorithms, a 3D image of the object can be constructed based on the projection data. In Figure 6.7 is presented the principle of 2D-tomography.

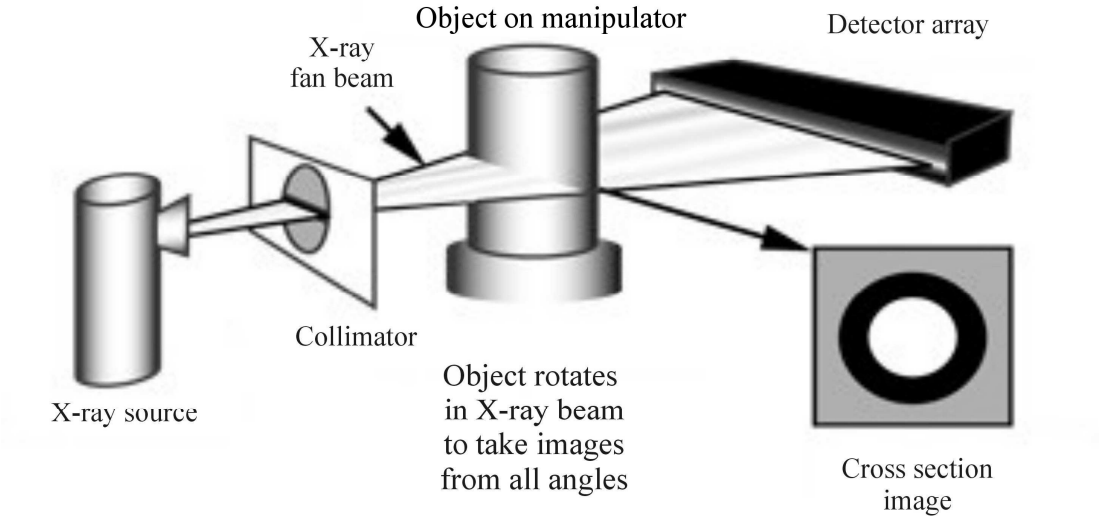

Figure 6.7 The principle of 2D-tomography. [14]

6.4 Image reconstruction

There are numerous ways to perform image reconstruction. The methods can be classified as:

- algebraic reconstruction technique (also known as series expansion methods),
- analytical reconstruction algorithms and

- statistical reconstruction techniques.

Algebraic reconstruction technique is the most simple image reconstruction technique. Filtered backprojection method is one of analytical reconstruction algorithms and it is most commonly used algorithm for tomographic reconstruction. Maximum likelihood method and maximum entropy are statistical reconstruction techniques.

6.4.1 Algebraic reconstruction technique

Information on the unknown distribution of attenuation coefficients is only given in form of a set of projection values, which are also termed the “Radon transform” of the image. In the context of tomography the Radon transform data is often called a sinogram. An inverse transformation has to be carried out to determine the distribution of attenuation coefficients. Different procedures are available to do this. The most easily understood approach to solve this problem is the following: N^2 unknown values, the N x N pixel value of the matrix, have to be computed by solving N_X independent equations, the measured projections. If N_X, the product of the number of the projections N_P times the number of data points per projection N_D, is larger than or equal to N^2 this is possible.

In the simplest case of an image matrix with only four pixels (2 x 2 matrix) two measurements for two projections will yield a system of four equations and four unknowns which can be solved easily. This is presented in Figure 6.8. The extension to a 3 x 3 matrix with nine unknowns can also be solved easily with twelve measured values. This method is so-called algebraic reconstruction technique (ART). The image is computed in an iterative fashion i.e. by repeating the calculation in an effort to improve accuracy with each step. For larger data volumes, finer image matrices and higher demand on image quality ART approaches led to unacceptably high computation times.

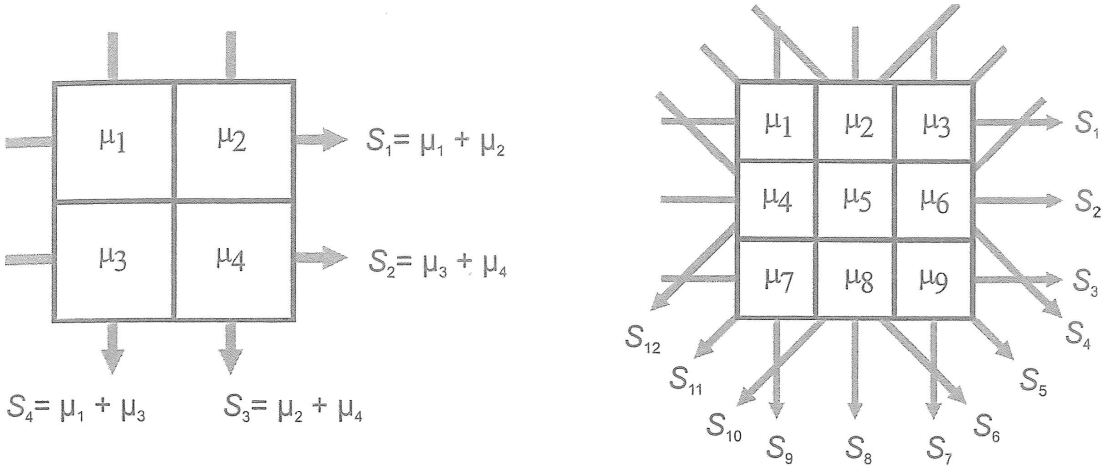

Figure 6.8 Principle of algebraic reconstruction technique.

6.4.2 Analytical technique

Filtered backprojection

The analytical methods are based on a mathematical solution to the problem how to reconstruct a function from its projections. Filtered backprojection method is one of analytical methods of image reconstruction and it is most commonly used algorithm for tomographic reconstruction.

After the measurement the projection data are available, and the image whose Radon transform corresponds to these measurement data is unknown. The first intuitive operation which can be implemented is backprojection. It consists in assigning to each point of the object the average value of all the projections at the corresponding location. The backprojected image, when compared with the “perfect object”, is highly blurred. As a result of the “projection-then-backprojection” process, each pixel contains information about what the object really contains at the pixel location, but this information is added to a blurred version of the rest of the object. An exact mathematical correction of the “projection-then-backprojection” smoothing can be done by an appropriate pre-filtering of the

projections, as in the filtered backprojection (FBP) algorithm. In Figure 6.9 is presented an example of reconstruction of an image using the filtered backprojection method.

Although filtered backprojection is popular in the field of image reconstruction, it has its disadvantages. One is the computational complexity which slows down the reconstruction process. Image quality can also be a problem. Small metallic objects may induce streaking artifacts on the reconstructed image. Compared to algebraic reconstruction techniques, filtered backprojection is not adaptable to missing data and partial occlusion effects.

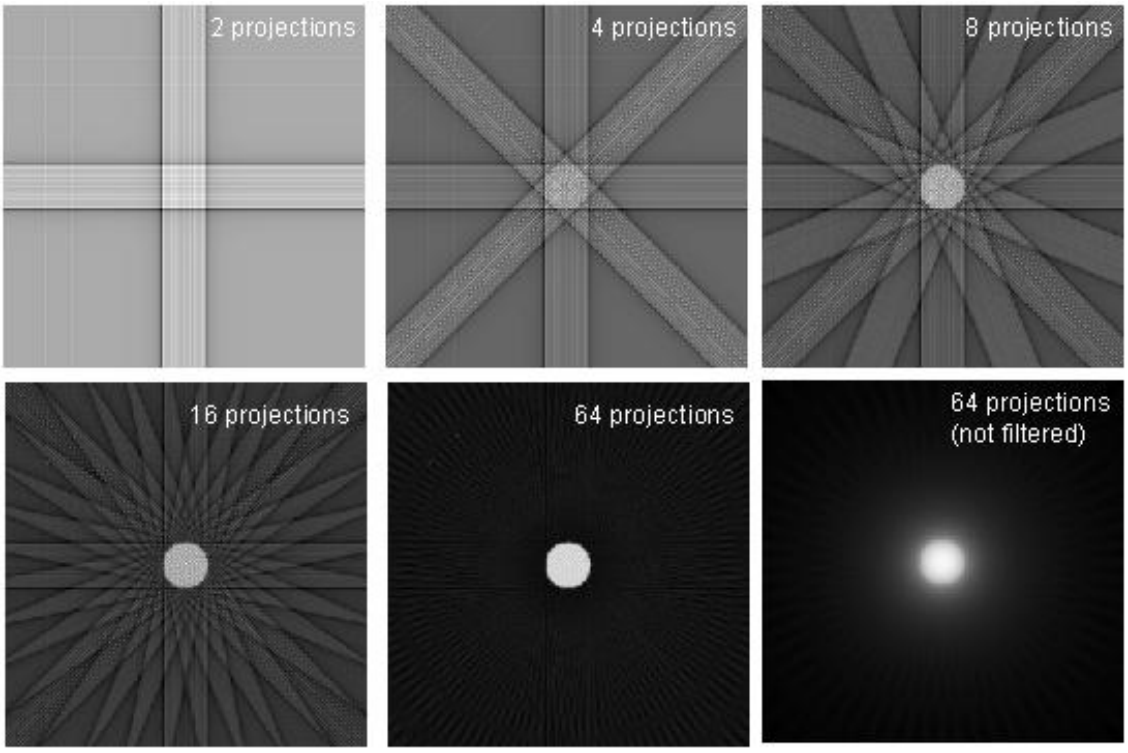

Figure 6.9 Reconstruction of an image using the filtered backprojection method. [13]

6.4.3 Statistical reconstruction techniques

Maximum likelihood method

Maximum likelihood method is a statistical estimation method used for fitting a mathematical model to data [20]. The image obtained is one that matches the measured projection values best, taking into account the measurement statistics of the real values. The measuring procedure must be modelled as a stochastic process whose parameters have to be estimated through a given random sample. Maximum likelihood method is typically used in situations where the number of quanta on the detectors is quite small and the sinogram therefore contains a lot of noise. In these cases, noise can dominate the reconstructed image if the algebraic or analytical methods for image reconstruction are used.

Maximum entropy

Maximum entropy is used as a technique for reconstructing positive images from noisy and incomplete data. An image can be regarded as a set of positive numbers which are to be determined, and on which the entropy is defined. The theoretical foundation of the maximum entropy method in data analysis is that this method is only consistent way of selecting a single image from the very many images which fit the data.

6.5 Image reconstruction artifacts

Reconstruction artifacts originate from a range of sources and they create artificial patterns inside the reconstructed slice (streak artifact) or they locally modify the pixels values (cupping effect) and thus the quantitative result.

Aliasing artifact or streaks

Aliasing artifact or streaks appear as dark lines which radiate away from sharp corners. It occurs because it is impossible for the scanner to “sample” or take enough projections of the object [20]. High spatial frequencies are encountered in the signal corresponding to every projection. They are due to a steep edges and sharp corners which are eventually present in the object. As the detector samples the signal (all along the projection) with a non-zero step, high frequencies corrupt the data, within the Fourier domain. Streaks are generated. This is typical for metallic objects. It can also occur when an insufficient electrical current is selected for an X-ray tube and insufficient penetration of the X-ray occurs. These artifacts are also closely tied to motion during a scan.

Partial volume effect

Partial volume effect appears as “blurring” over sharp edges. It is due to the scanner being unable to differentiate between a small amount of high density material and a larger amount of lower density. It occurs where the object does not fill scan plane. The processor tries to average out the the densities or structures and information is lost. This can be partially overcome by scanning using thinner slides.

Ring artifact

Ring artifact is probably the most common mechanical artifact. One or many “rings” appears within an image. This is due to a detector fault.

Noise artifact

Noise artifact appears as graining on the image and is caused by a low signal to noise ratio. This occurs more commonly when a thin slice thickness is

used. It can also occur when the electrical power supplied to the X-ray tube is too low.

Motion artifact

This artifact is seen as blurring which is caused by object movement. This is not a problem these days with faster scanning times in the use of multi detector computed tomography.

Windmill

Streaking appearances can occur when the detectors intersect the reconstruction plane. This can be reduced with filters or a reduction in pitch.

Beam hardening

As an X-ray source delivers a polychromatic spectrum, differential attenuation of photons within the investigated objects leads to the rapid attenuation of the lowest energy photons and thus to the gradual increase of the mean energy along the path. The reconstruction algorithm uses for the reconstruction of any single point experimental data corresponding to individual rays impinging the point of interest but coming from different orientations. The corresponding information therefore corresponds to different attenuations and thus different energies and different values of attenuation. Two kinds of artifacts are generated by beam hardening: 1) cupping effect and 2) streaks. Cupping effect corresponds to measured values of attenuation which are corrupted thus preventing the measurement of the “true” density. As the measured values, inside a homogenous sample, are lower at the center than at the edges, the cupping effect occurs. Projections can be corrected by acquiring an image of a step-wedge, made of the same material, in such a way to correlate the measured attenuation to the material thickness. Streaks artifact correspond to abnormal values along lines which correspond, inside the object, to high attenuation. The beam

hardening effect is shown in Figure 8.3. Beam hardening artifacts can be avoided when using some filter i.e. a metallic foil directly set at the window at the X-ray tube and intended to pre-harden the spectrum [20]. Beam hardening is also avoided when using a monochromatic gamma-ray source. But the problem is that gamma-ray sources deliver a very low photon flux (typically one hundredth of the flux delivered by an X-ray tube).

Centering error

The reconstruction requires the knowledge of the location of the projection of the center of rotation within the detector. Distortions are generated when the reference to the centre is defective.

Detector saturation

To obtain a reconstruction which is free of errors the signal delivered by every cell of the detector must be strictly proportional to the photon flux. Thus high values (approaching the upper limit of the digitization range) as well as low values (approaching the noise level) of the flux must be avoided. Streaks artifacts are generated along lines which correspond to high attenuation.

Spatial distortion of the detector

Distortions of the projections, due for instance to the camera (e.g. distortions due to the lens) deliver artifacts which can be corrected by software.

Scattered photons

Photons scattered by the sample or by its environment deliver detective information which leads to cupping effect. Collimation can improve the reconstructed image.

7. Gamma emission and X-ray transmission tomography of nuclear fuel

7.1 Gamma emission tomography of nuclear fuel

The operational principle, measuring methods and mechanical arrangements of gamma emission tomography of nuclear fuel are similar to gamma spectrometry of nuclear fuel. The gamma-ray spectrum of irradiated nuclear fuel is recorded for several projections and with this information image is reconstructed.

Only isotopes with a half-life longer than a few days can be utilized because the measurements cannot be performed in-core. The isotopes should emit gamma radiation of sufficient energy to escape from the fuel. The higher the gamma-ray energy, the more information can be obtained from the inner sections of the fuel. In table 7.1 are presented the isotopes that can be used in gamma emission tomography measurements of nuclear fuel (gamma energy higher than 600 keV).

Table 7.1 Isotopes that can be used in gamma emission tomography measurements of nuclear fuel (gamma energy higher than 600 keV).

Isotope	Gamma energies [keV]	Half-life	Relevant cooling time
^{140}Ba (^{140}La)	1596	12.8 d	<50 d
^{95}Zr (^{95}Nb)	724, 757, 766	64 d	30 d-0.5 y
^{144}Ce (^{144}Pr)	696, 2186	284 d	0.3-2 y
^{134}Cs	605, 796	2.1 y	1-10 y
^{154}Eu	1274	8.5 y	2-30 y
^{137}Cs	662	30 y	2-100 y

A basic requirement of a device for tomographic measurements is the ability to record the gamma radiation in a large number of positions relative to the measured object. In each position, gamma-ray detectors are used for collecting information about the gamma flux. Because irradiated nuclear fuel assemblies contain a variety of radioactive isotopes, the data-acquisition system should be able to distinguish between the radiation of interest and other radiation.

7.2 X-ray transmission tomography of nuclear fuel

7.2.1 Principle

A radiation source (X-ray tube or linear accelerator) with adequate collimation emits a beam and the intensity, attenuated by the nuclear fuel assembly, is registered by the detectors placed opposite. For a given position, the nuclear fuel assembly is moved linearly (translation) or helically, and the intensity is measured either at single discrete points or continuously. This result in an intensity profile recorded for parallel rays. By determining the ratios of the primary intensity recorded in the periphery and attenuated intensities recorded behind the nuclear fuel assembly and taking their logarithms, an attenuation profile results, which is generally termed a projection. The complete set of projections is then transferred to the data processing unit, where the image is reconstructed. The principle of transmission tomography is presented in Figure 6.5.

High-energy X-ray applications for radiography testing and computerized tomography on large or dense objects require X- or gamma-rays of at least 1 MeV to reach sufficient signal to noise ratio in attenuation measurements. These high-energy photons are produced either by a ^{60}Co isotropic source (as a monochromatic continuous beam) or by a linear accelerator of

electrons (also called a linac) coupled with a Bremsstrahlung target (polychromatic pulsed beam).

X-ray transmission tomography of nuclear fuel can be used in following applications:

- Before an irradiation (receipt checking)
  - General status after transportation
  - Location of instrumentation.

- After an irradiation or a damaging test
  - First view of a fuel sample
  - Dimensions or geometry evolutions.

- Support to scientific objectives of the experiment
  - Metrology (fissile stack elongation and fuel densification)
  - Detailed fuel morphology (cracks, dishing, etc.).

7.2.2 X-ray tube

In a vacuum tube, there is an emitter, either a filament or cathode, which emits electrons into the vacuum and an anode to collect the electrons through the tube. This flow of electrical current is known as the beam. A high voltage power source is connected across cathode and anode to accelerate the electrons. Electrons from the cathode collide with a metal target (usually tungsten and sometimes molybdenum or copper) deposited on the anode and accelerate other electrons within the deposited material. X-rays are produced when the electrons are suddenly decelerated upon collision with the metal target. These X-rays are commonly called Bremsstrahlung. X-rays can also be produced as characteristic X-rays. In Figure 7.1 is presented a schematic drawing of an X-ray tube. In medical diagnostics and radiation therapy acceleration voltages are chosen between 25 kV and 300 kV, and for material testing they can reach up to 500 kV.

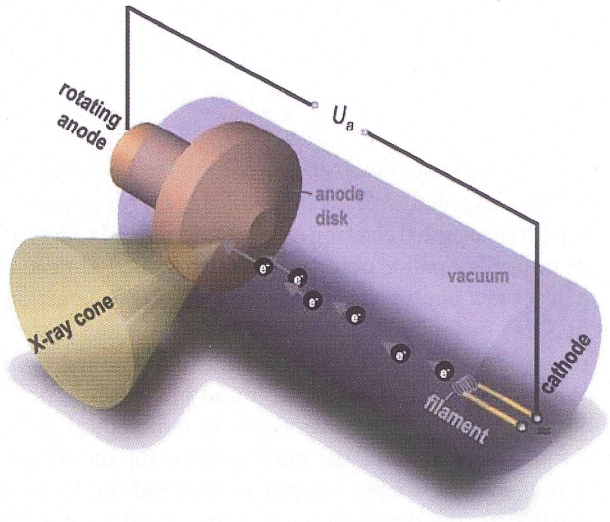

Figure 7.1 Schematic drawing of an X-ray tube. [20]

7.2.3 Linear accelerator

A linear accelerator is an electrical device for the acceleration of subatomic particles. The design of linear accelerator depends on the type of particle that is being accelerated: electron, proton or ion. Electrons are generated by a cold cathode, a hot cathode, a photocathode, or a radio frequency (RF) ion sources.

RF linear accelerator uses microwave energy to accelerate electrons. The accelerated electrons stroke a metal target to produce X-rays. Because the required RF power to set up these accelerating fields is so high (typically megawatts), the power can be produced only in very short pulses, typically 5 to 10 μs. The pulsed RF energy (typical frequencies 3 to 10 GHz), is developed in special microwave RF generator tubes. These microwave tubes require high voltage pulses and hundreds of amperes of current to operate. The pulses to operate the microwave generators are created in a device called modulator. The modulator requires high voltage direct current (DC) which is produced in a high voltage supply. This is either part of the modulator or a separate system.

In high energy X-ray radiography, a radio frequency linear accelerator is used as a high energy X-ray source. In radio frequency linear accelerator, the electric field component of radio waves accelerates particles inside a partially closed conducting cavity acting as a radio frequency cavity resonator. The linear accelerator, which is used for non-destructive testing (NDT) applications, typically has X-ray energies from 1 to 20 MeV.

Parts of linear accelerator:

- High voltage supply (produces high voltage required for proper modulator operation)
- Modulator (provides high voltage pulses to the microwave generator)
- Radio frequency source system (converts high voltage pulses from the modulator into pulsed radio frequency energy)
- X-ray system (applies RF to the accelerating structure to accelerate electrons and produce X-rays)
- Auxiliary systems (automatic frequency control, energy change and dose monitoring).

In Figure 7.2 is presented the structure of linear accelerator.

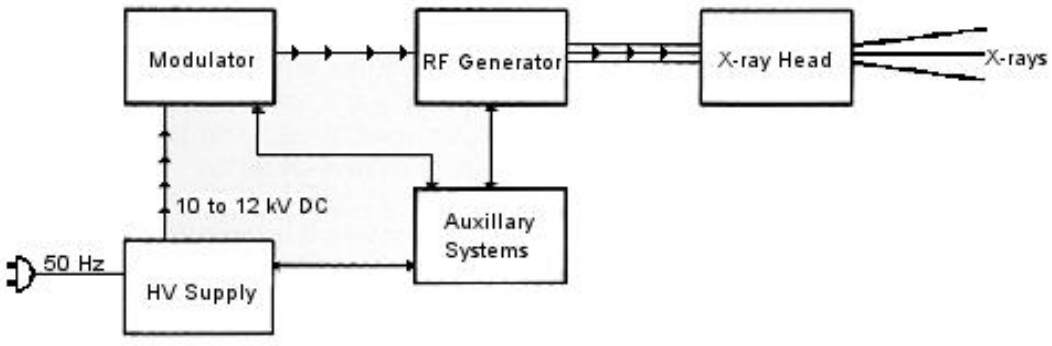

Figure 7.2 Structure of linear accelerator.

Very important linear accelerator parameter is X-ray spot size, which determines the imaging capability of the linear accelerator. There is a design limitation on minimum spot size due to scattering of electrons in the target material. In the typical thick target design, the smallest X-ray spot achievable is between 0.25 and 0.5 mm. In this case the thickness of the target is slightly greater than the penetration depth of the electrons. It is possible to get smaller spot sizes using “thin” target design. It is important to ensure that any electrons which pass through the target are trapped in some manner, either by a magnetic field or in a low density material such as carbon.

7.3 Detectors

Four main detector types can be found in the field of tomography:

- gas ionisation detectors were used in the early medical scanners. Their main characteristic is their high dynamic range. Filled with gas having a high atomic number, they can be used even with high energies.
- image identifiers (I.I.) are used in small and portable scanners for industrial non-destructive testing (NDT) of small components. Their disadvantages are low dynamic range and inherent distortion of the image.
- scintillation detectors, composed of a fluorescent material (e.g. gadolinium oxysulphide Gd_2O_2S, or cesium iodide CsI) are nowadays widely used. Those detectors are two of kinds: 1) the fluorescent material is directly coupled into to an array of photodiodes or of photomultipliers, 2) the fluorescent material is spread on a screen which is optically coupled to a charge-coupled device (CCD) camera via a lens.
- arrays of semiconductors (e.g. cadmium telluride (CdTe) or cadmium-zinc-telluride CZT), which allow a direct photon detection. High energy applications are possible for this type of detectors.

7.4 Mechanical arrangement

Typically the tomographic measurements are made with same mechanical equipment than gamma spectrometry measurements. The detectors are placed in watertight container or similar and they are submersed into the pool. X-ray source is positioned other end of the collimator and X-ray beam is collimated precisely. X-ray tomography can also be performed in high activity cell. In Figure 7.3 is presented the measurement system for gamma emission and X-ray transmission tomography of nuclear fuel.

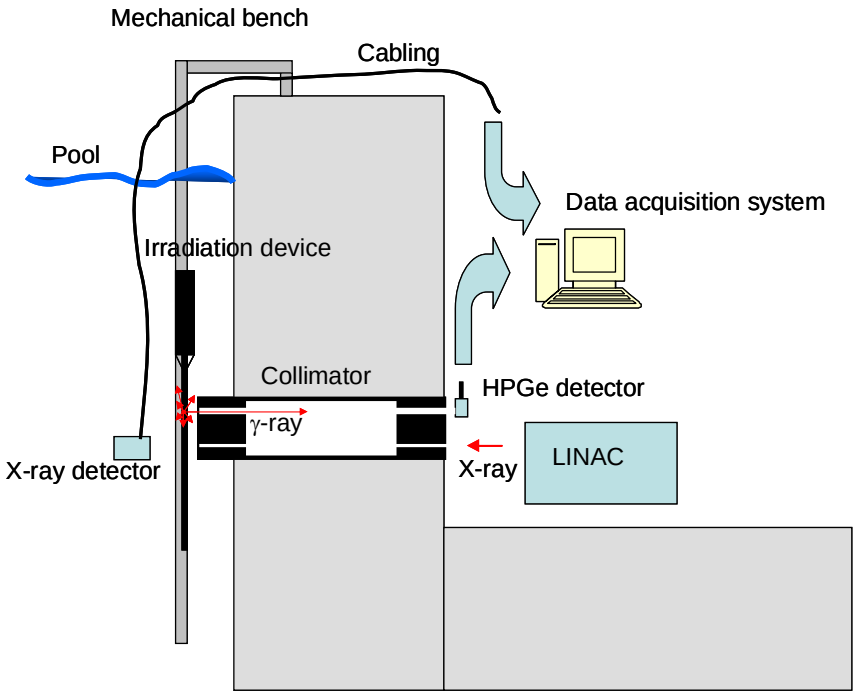

Figure 7.3 Measurement system for gamma emission and X-ray transmission tomography of nuclear fuel.

7.5 Advantages and disadvantages

Typically the tomographic measurements are made with same mechanical equipment than gamma spectrometry measurements. For that reason problems related to nuclear fuel and mechanical structures are quite similar

than in gamma spectrometry of irradiated nuclear fuel (high activity of irradiated nuclear fuel, absorption of gamma radiation, complexity of spectrum coming from the measurements of irradiated fuel, etc.).

The biggest problems are related to image reconstruction. The problems are presented in chapter 6.5.

8. MODHERATO

8.1 Principle of the MODHERATO code

MODHERATO (“Modélisaton Haute Energie pour la Radiographie et la Tomographie” or in English “Modelling High Energy Radiation Tomography”) is a computer code that was developed to simulate the operation of radioscopic or tomographic devices. This code can be helpful to predict and optimise the performance of imaging system. The whole geometry of the system from the source to the detector can be defined and monochromatic or polychromatic beams can be chosen.

MODHERATO uses the results of Monte-Carlo N-Particle Transport Code (MCNP) in electron-photon mode to describe the X-ray beam generated by accelerated electrons within a Bremsstrahlung target as a function of the energy and the angle ($\Phi(E,\theta)$) This statistical code has permitted to optimize the thickness of tungsten target in order to increase photonic production.

Ray-tracing techniques together with the X-ray attenuation law are the basis of the MODHERATO code. From each source point a set of rays is emitted towards every pixel centre of the detector. Each ray may intersect a certain number of meshes on the object surface. The attenuation path length in every object phase is calculated by determining the coordinates of all intersection points. The photon number *N(E)* that emerges from the sample and reaches the detector surface is given by the attenuation law:

$$N(E) = \sum N_0(E) e^{-\sum_i \mu_i(E) * x_i} \quad (5)$$

As a result is an electronic signal as a function of dose rate.

MODHERATO takes into account statistical noise, geometrical blurring effect and detection dynamic range to simulate physical phenomena and electronics behaviour which affect the attenuation measurements. In Figure 8.1 is presented the structure of MODHERATO code.

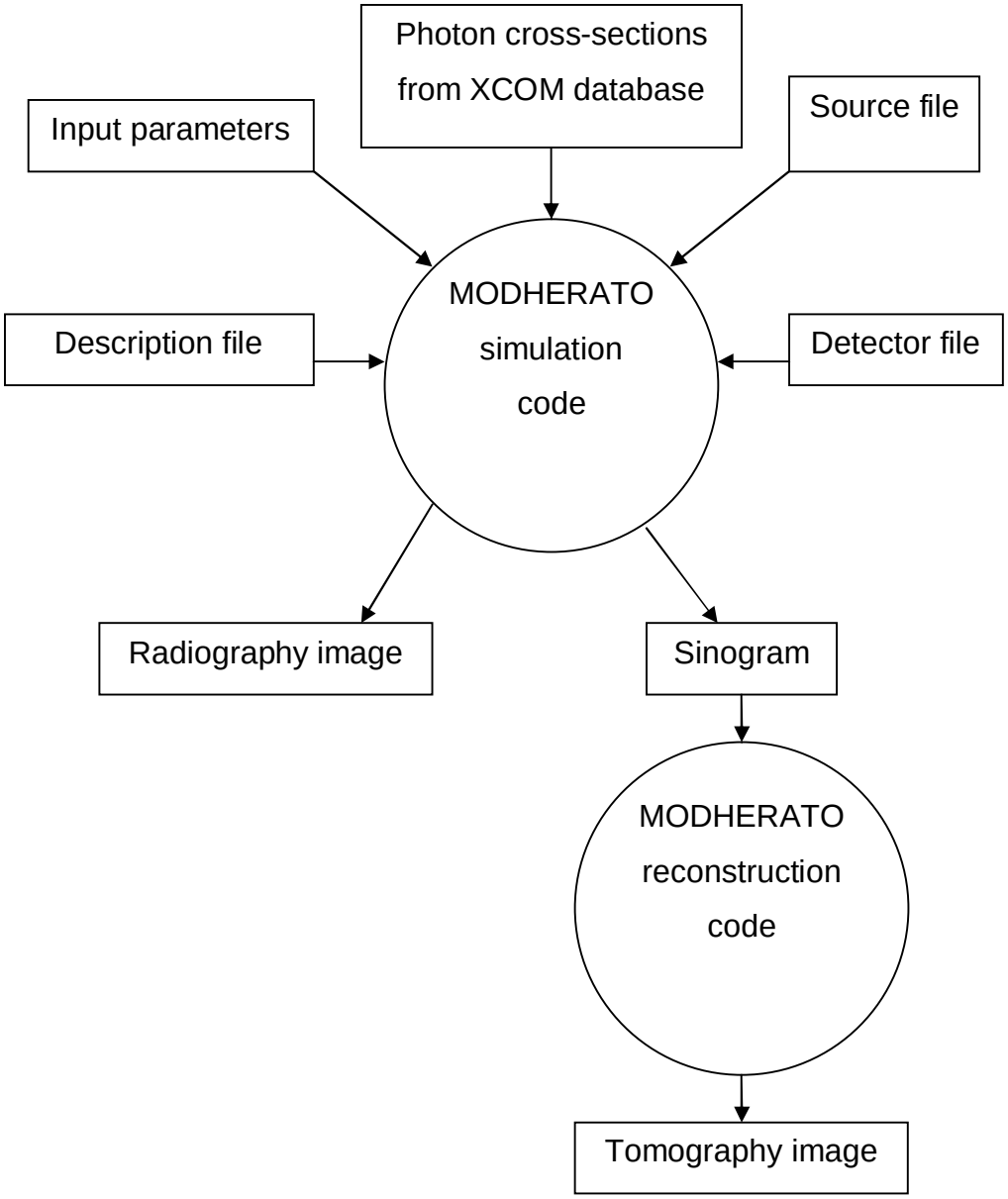

Figure 8.1 Structure of MODHERATO code.

Descriptions of different components of the MODHERATO code follows.

Description file

The volumes and objects to be measured are determined in this file

Photon cross-sections from XCOM database

Database can be used to calculate photon cross-section for scattering, photoelectric absorption and pair production, as well as total attenuation coefficients for any element, compound or mixture (Z<100) at energies from 1 keV 100 GeV.

Input parameters

The measuring method is described in input parameter file. Radiography, 2D-tomography or 3D-tomography can be chosen.

Source file

Determines the characteristics of the radiation source (shape, size, position, orientation, etc.).

Detector file

Determines the characteristics of the detector (position, orientation, pixel number and size, etc.).

8.2 Results of MODHERATO simulations

Simulated objects were a barrel surrounded by water and three rods which were inside the barrel. The rods consisted of either iron or uranium dioxide. In Figure 8.2 a radiography image and in Figure 8.3 2D-tomography image of

the objects is presented. Either X-ray tube or linear accelerator was used as an X-ray source.

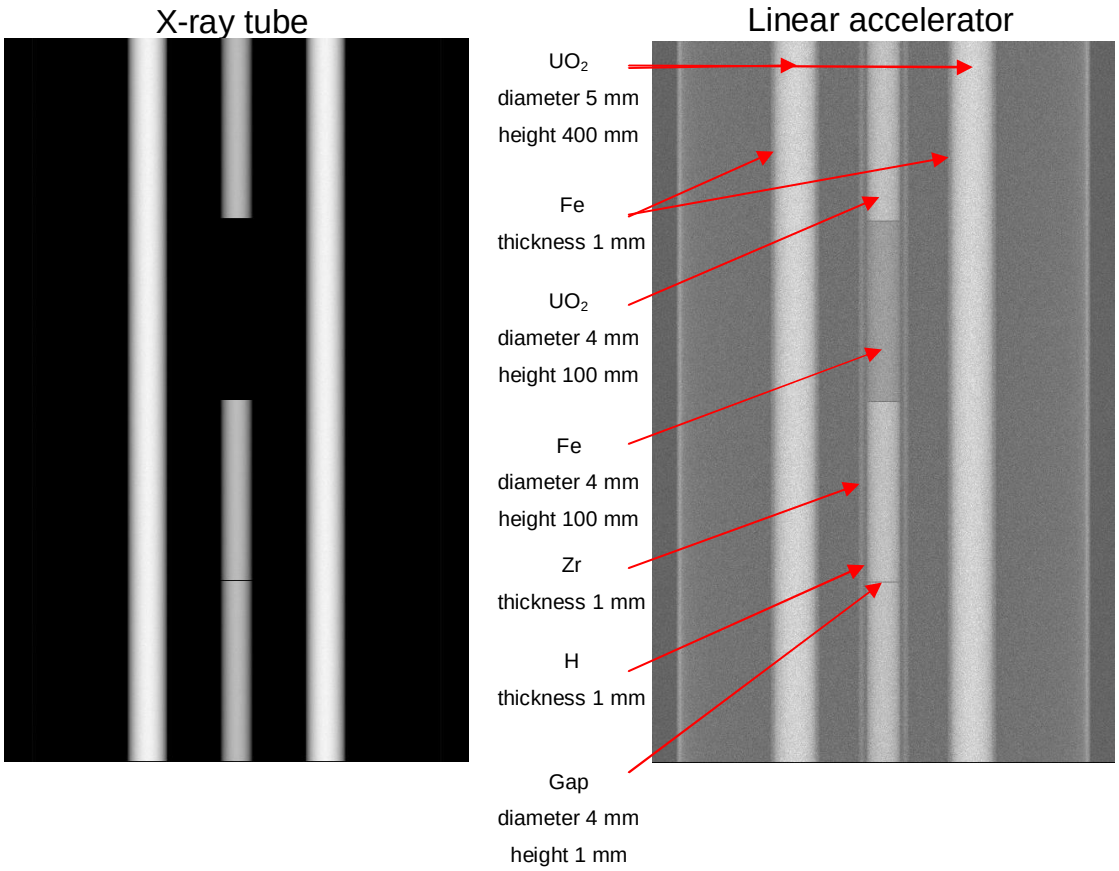

Figure 8.2 Radiography with X-ray tube or linear accelerator.

Figure 8.2 shows the difference between two different X-ray sources. The edge of the barrel is clearly visible in radiography image on the right side (linear accelerator). Differences between different material densities are also visible on the right side in Figure 8.2.

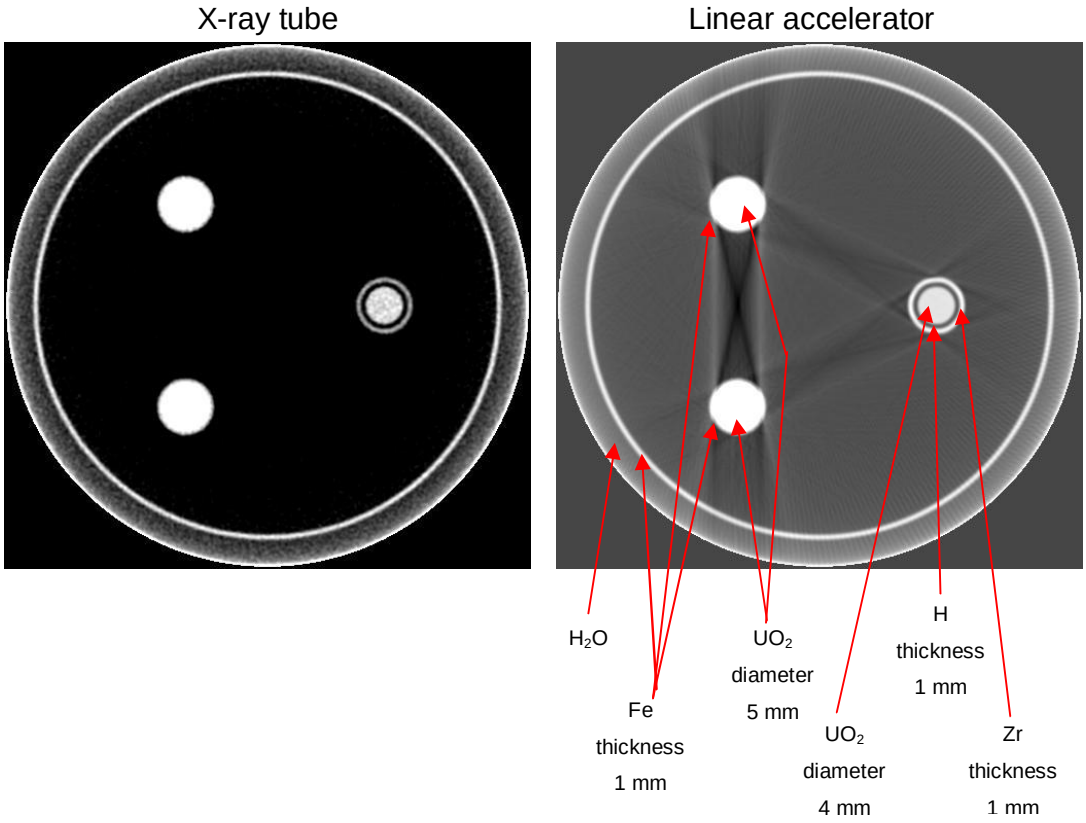

Figure 8.3 2D tomography with X-ray tube or linear accelerator.

Streak artifacts caused by beam hardening are visible on the right side (linear accelerator) in Figure 8.3. Streaks correspond to abnormal values along lines which correspond, inside the object, to high attenuation.

By comparing simulation results obtained at different X-ray sources or X-ray tube voltages it is possible to predict the more favourable energy leading to optimal image quality in any specific application. For example when the photon energy raises the quantity of transmitted photons is more important and the relative photon noise is smaller. However the image contrast is lower and therefore a compromise has to be found. To determine the latter simulation can be a helpful tool.

9. Some existing equipment used for gamma spectrometry and/or tomography of nuclear fuel

9.1 Clab, Sweden

At Clab and all Swedish BWR reactors, installations that can be used for gamma spectrometry and gamma emission tomography measurements are available. The equipment is not optimized for gamma scanning method but is used so far since it is easily available. The system measures ^{137}Cs intensity to determine the decay heat and ^{137}Cs, ^{134}Cs and ^{154}Eu intensities to determine burnup, cooling time and the axial isotope distribution [22].

At the stationary installation a fixture for the fuel assembly is mounted on the pool wall. The fixture can be moved vertically by an elevator and rotated around its own axis in a large amount of small steps by a stepper motor. The vertical speed as well as the rotational speed can be changed by the operator. The germanium detector is mounted inside the pool wall and a collimator is placed to the other side of the wall. The collimator is 120 cm long and wide enough to cover the diagonal width of a fuel assembly. It is made of two massive steel half cylinders. The purpose of the collimator is to allow the radiation from the full diagonal of the fuel assembly to reach the detector. The height of the collimator can be varied between 1, 2 and 3 mm. This height is used to adjust the counting rate in the detector. The distance from the centre of the fuel assembly to the end of the collimator is about 250 cm. At the back end of the collimator, a lead filter and a copper plate are placed to filter away low-energy gamma rays that otherwise would load the detector system with unnecessary radiation for this application.

When a fuel assembly is about to be measured it is placed in the fixture, which is at its starting position a bit below the collimator slit. The fixture is then placed in the desired angular starting position and measurement can

start. By moving the fixture upwards in front of the horizontal collimator slit the whole length of the fuel is scanned.

More information about Clab can be found from Ref. [22].

9.2 LOKET, Sweden

LOKET is designed for measurements at nuclear power plants lacking the through-wall collimator option and it can be submersed into a fuel handling pool [11]. The measurements are performed at a water depth of about 7 m. The detector is shielded using lead and a tungsten alloy (densaloy). The steel collimator is about 1 m in length with a slit height of 1-5 mm. The slit width can be varied from a few cm at the detector end to more than 20 cm at the fuel end for assembly measurements. To be able to adjust the counting rate in the detector, the gamma ray intensity from the measured object is reduced by inserting a suitable tungsten alloy attenuator in front of the detector. The detector used is a high-purity germanium p-type detector cooled with liquid nitrogen through a side looking dewar mounting and with approximately 25 % relative efficiency. In Figure 9.1 is presented the principal experimental set-up for measurements using the submergible detector system LOKET.

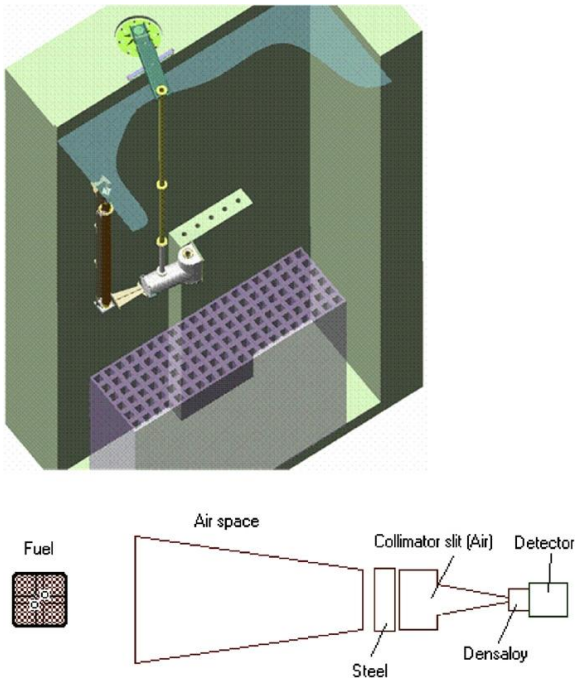

Figure 9.1 The principal experimental set-up for measurements using the submergible detector system LOKET. [11]

9.3 Fork, Finland

This equipment is based on a standard IAEA BWR fork detector concept with a special upgrade, which integrates into the device a cadmium-zinc-telluride (CZT) detector and a collimator assembly for gamma spectroscopic measurements [12]. The fork detector head consists of four fission chambers for neutron detection and two ionisation chambers for gross gamma measurement. The detectors are positioned symmetrically inside two detachable polyethylene prongs, which are on opposite sides of the assembly to be measured. The opening between the prongs is nominally 149 mm whereas the thickness of the assembly with a fuel channel is nominally 139 mm. The detector head forms a closed watertight package.

An 8 m long vertical pipe consisting of four 2 m long sections holds the detector head during the measurements and brings the dry cables from the pool to the floor level. An extra 1 m long section is provided to adjust the height of the vertical pipe at 1 metre intervals (7, 8 or 9 metres). The vertical

pipe is fixed in the periscope console in the edge of the pool. In Figure 9.2 is presented the structure of the fork detector.

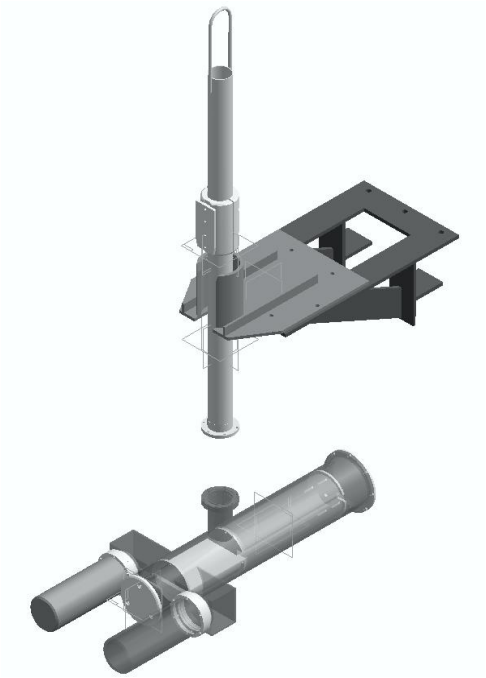

Figure 9.2 The structure of the fork detector. [12]

10. Conclusions and recommendations

In this work, gamma spectrometry, X-ray radiography, and gamma and X-ray tomography methods have been reviewed. Related to the X-ray tomography, MODHERATO simulations have been performed by the author.

Gamma spectrometry, radiography, and gamma and X-ray tomography are promising examination methods for understanding fuel behaviour under normal, transient and accident conditions. Gamma spectrometry and tomography are also important methods in safeguards and verification of nuclear fuel.

Due to properties of irradiated nuclear fuel and the type of its gamma emitters, a rather complex implementation is required, both for the acquisition of spectra and their analysis and interpretation.

Detector

Semiconductor detectors are commercial products and manufacturers do not have interest to develop detector only for measurements of irradiated nuclear fuel because these measurements represents a minority of the gamma spectrometry measurements.

Large number of peaks from different decays makes high resolution desirable in order to select the decay of interest. An optimum would be to use detectors with high resolution and high peak efficiency together with spectroscopic analysis. However, both high resolution and high peak efficiency may be difficult to achieve in practice.

In gamma emission measurements HPGe detectors are superior due to their high energy resolution. In X-ray transmission measurements, good high speed particle detection efficiency is desirable. Recent development of

semiconductor compound detectors has shown that their characteristics are excellent for X-ray transmission measurements. For example, the high electron mobility in GaAs, offers the prospect of high speed particle detection and signal processing.

Collimator

Typically the collimator is made of iron or steel because of their low cost. However there are better collimator materials available e.g. tungsten due to its much higher atomic number.

Mechanical bench

The nuclear fuel to be measured should be positioned laterally and angularly with accuracy within a few millimeters and one degree. These requirements are challenging to the design of the mechanical bench. Excellent performances of the detector and the X-ray source will be forfeited if the accuracy of the mechanical bench is poor. Accurate design should be emphasized.

Image reconstruction

At the moment the filtered backprojection method is the best mathematical reconstruction method available for tomography of nuclear fuel. However there are also other image reconstruction methods that can be used for the tomography of the nuclear fuel, e.g. statistical maximum likelihood and maximum entropy methods, which are needed if the measured data contains a lot of noise.

Good scanner design, careful positioning of the object and optimum selection of scan parameters can minimise the artifacts present in an image.

References

[1] Knoll, G. Radiation Detection and Measurement. Second edition. John Wiley & Sons (1989).

[2] Gilmore, G. & Hemingway J. Practical Gamma-ray Spectrometry. Chichester. John Wiley & Sons (1995).

[3] International Atomic Energy Agency. Power Reactor Information System [web document]. Published 10th May 2000, updated 19th March 2009 [referenced 23th February 2009]. Available:http://www.iaea.org/programmes/a2.

[4] CEA. The Nuclear Fuel of PWR's and FR's: Design and Behaviour. Lavoisier Publishing (1999).

[5] Ikäheimonen, T (Ed.). Säteily- ja ydinturvallisuus: Säteily ja sen havaitseminen. Säteilyturvakeskus (2002).

[6] Glasstone, S. & Sesonske, A. Nuclear Reactor Engineering. Krieger Publishing Company, Malabar, Florida (1981).

[7] Fink, J., Chasanov, M. & Leibowitz, L. Thermodynamic Properties of Uranium Dioxide. Journal of Nuclear Materials, vol. 102, pp. 17-25 (1981).

[8] Radon, J. Über die Bestimmung von Funktionen durch ihre Integralwerte längs gewisser Mannigfaltigkeiten. Ber vor Säch. Akad Wiss. 1917; 69: 262-277. (English translation available: Radon, J. On Determination of Functions from Their Integral Values Along Certain Manifolds. IEEE Transactions on Medical Imaging 196; MI-5(4): 170-176).

[9] Pettier, J-L. 2007. PhD. CEA. Personal discussion 10 November 2007.

[10] Pfennig, G., Klewe-Nebenius, H. & Seelmann-Eggbert, W. Karlsruher Nuklidkarte. Forschungszentrum Karslruhe GmbH (1998).

[11] Matsson, I., Grapengiesser, B. & Andersson, B. LOKET- a gamma-ray spectroscopy system for in-pool measurements of thermal power distribution in irradiated nuclear fuel [web document]. Uppsala University. Department of Nuclear and Particle Physics. Published 2006 [referenced 23rd October 2007]. Available: http://www.sciencedirect.com/science?_ob=ArticleURL&_udi=B6TJM4M5WPFG2&_user=61181&_coverDate=12%2F21%2F2006&_alid=886892973&_rdoc=2&_fmt=high&_orig=search&_cdi=5314&_sort=d&_docanchor=&view=c&_ct=5&_acct=C000005398&_version=1&_urlVersion=0&_userid=61181&md5=a2e063a1a202201354db0d9ccf4e5d4d.

[12] Tiitta, A. et al. Spent BWR fuel characterisation combining a fork detector with gamma spectrometry: Raport on Task JNT A 1071 FIN of the Finnish Support Programme to IAEA Safeguards. Säteilyturvakeskus (2001).

[13] Platten, D. Multi-slice Helical CT Physics and Technology [web document]. A UK Department of Health: MHRA Device Evaluation Group. Published 2003 [referenced 20th January 2009]. Available: http://www.impactscan.org/slides/eanm2002/sld014.html.

[14] University of Liege, Laboratory of Chemical Engineering, Department of Applied Chemistry. High Energy X-ray Tomography [web document]. Updated 6th July 2008 [referenced 11th November 2008]. Available as PDF-file: http://www2.ulg.ac.be/bioreact/RX420.pdf.

[15] Walker, C. et al. Concerning the microstructure changes that occur at the surface of UO_2 fuel pellets in irradiation to high burnup. Journal of Nuclear Materials, vol. 188, pp. 73-79 (1992).

[16] Franklin, D. et al. Low temperature swelling and densification properties of LWR fuels. Journal of Nuclear Materials, vol. 125, issue 1, pp. 96-103 (1984).

[17] Massih, A. Fission Gas Release. ABB Atom Report BKC 94-010 (1994).

[18] CEA. First technical requirements for underwater gamma spectrometry and X-ray imaging system in the JHR facility. Technical report draft issue 1 November 2006.

[19] Wikipedia. Beer-Lambert Law [web document]. Updated 14th March 2009 [referenced 25th February 2009]. Available: http://en.wikipedia.org/wiki/Beer-Lambert_law.

[20] Buzug, T. Computed Tomography: From Modern Statistics to Modern Cone-Beam CT. Springer-Verlag. Berlin (2008).

[21] Kalli, H. Lappeenranta university of technology. Department of energy technology. Ydinreaktorien fysiikka: osa I. (2001)

[22] SKB. Clab-en tillbakablick på byggprojektet [web document]. Referenced 7th April. Available as PDF-file: http://www.skb.se/upload/publications/pdf/SKB_clab_historia_20081209.pdf.